# Observing double-Weyl points in ultracold atoms by Landau-Zener transitions and Stückelberg oscillations

## Bachelor Project

Written by

*Magnus Rønne Lykkegaard*

Supervised by

*Michele Burrello*

UNIVERSITY OF COPENHAGEN

FACULTY: Science

INSTITUTE: Niels Bohr Institute

AUTHORS: Magnus Rønne Lykkegaard          KU-ID: CXW938

TITLE: Observing double-Weyl points in ultracold atoms by Landau-Zener transitions and Stückelberg oscillations

SUPERVISOR: Michele Burrello          michele.burrello@nbi.ku.dk

HANDED IN: 12$^{th}$ of June 2019

DEFENDED: 4$^{th}$ of July 2019

**Abstract**

This thesis study an ultra cold (UC) atom trap simulation of a topological semi-metal with double-Weyl points in a cubic lattice. Atoms in the simulated topological semimetal system can be driven by external forces through the Brillouin Zone (BZ), and as such the population in the two-level system of the effective Hamiltonian, can be examined. Especially the evolution close to the band-touching points, where non-adiabatic transitions, Landau-Zener transition, take place is of great interest. The double-Weyl semimetal quadratic energy dispersion is special compared to that of the linear dispersion that single-Weyl semimetals has. The quadratic dispersion is compared with that of the standard Landau-Zener problem, a linear dispersion, which is also present in the system. The system has more than one Weyl point, and therefore more than one transition. Therefore the two-band populations undergo Stückelberg oscillations. The goal is to present a first order computation, and predict the results of a potential future experiment.

A description of the topology of the Weyl points is studied as a description of the anomalous flow that the system undergoes in real space. We find that no flow is present in our case. The discussion of realizing the Hamiltonian in experiments is described as well as a discussion of the diabatic case. Furthermore, higher order calculations are also presented.

# Contents

# 1   Introduction

The theory of exotic topological quantum matter have enjoyed a growing interest in the last decade. Though they have previously been studied in solid state sytems, the advent of quantum simulations using ultra cold (UC) atom traps has sped up the study [1]. Observables, which are not studied in solid state physics of these theoretically predicted states of quantum matter, can be accessed within a controlable environment of high tunability. This thesis' goal is to achieve an understanding of one such quantum matter's transport properties: The double-Weyl semimetal.

Topology in mathematics is the description of equivalency in geometry. In the physics of topological semimetals the word refers to the stability of the band structure. Topological semimetals are a gapless state of matter with a stable Fermi surface. Several types of topological semimetals exist, and the Weyl semimetal is one of the canonical examples of these. The band touching points are protected and described by the topological invariance of the Chern number of the points. This invariance, which is the topological charge of the system, can be violated by breaking the symmetries of the Hamiltonian. Breaking the $C_4$ rotational symmetry invariance, will result in splitting the double-Weyl into two Weyl points of charge $\pm 1$. Double-Weyl point can be brought together to annihalate each other. Keeping the Weyl points far from each other will therefore, be key to the stability of the band structure. If the double-Weyl point is situated at the Fermi surface it will result in a hole in the surface, constituting a incomplete Fermi surface, and exotic surface arc states will appear, which have an intrinsic chirality. The wavefunctions link two nodes of different chirality [2, 3].

Using a low energy effective Hamiltonian of a cubic Bloch band lattice structure enables the approximation of a two state system. We will adapt the following notation for derivatives,

$$\partial_i^n = \frac{\partial^n}{\partial^n i} \tag{1.1}$$

and the natural constant of $\hbar = 1$.

## 1.1   Realizing the cubic lattice of a Weyl semimetal in an UC atom trap

The modeling of the double-Weyl Hamiltonian and its lattice structure in a UC atom traps is not the main objective of this thesis. However, for the sake of completeness, I summarize the main features of the proposal presented in [4] for the realization of a double-Weyl semimetal based on an UC atom system in an optical lattice subject to artificial gauge potentials. Articifial gauge fields are an enormously valuable tool to simulate magnetic fields. When the internal states, in this case there are two, couple they generate lattice vortices that are synonymous to magnetic vortices [5]. Because of the energy difference between neighbouring lattice sites, Raman lasers with a frequency equal to the energy difference couple them [6]. This in turn constitute vortices in all unit cells, which is the simulation of an extremely large magnetic field.

To find an effective low-energy Hamiltonian for the two-level system, firstly a system with Weyl nodes is

defined, by introducing the Abelian, Hasegawa gauge $A_{AB}$ [4, 7], that establish $\pi$ pulses in the lattice at the postion $\mathbf{r} = (x, y, z)$,

$$\mathbf{A}_{AB}(y, z) = \mathcal{I}_{2 \times 2} \pi \begin{pmatrix} z - y \\ y - z \\ 0 \end{pmatrix}. \tag{1.2}$$

Note that two states or species of an atom are accounted for in the gauge of Eq. 1.2 by the 2 by 2 identity matrix, $\mathcal{I}_{2 \times 2}$. Otherwise physically achievable species of spin, has been shown to be energetically unfavorable in an experimental setup [5, 6]. The species are regarded as a hyperfine structure of the system, which is degenerate in the ground state manifold [5]. The manifold is defined by the topology of the system's Berry curvature [8]. The topology of the system will also be described in this thesis' Sec. 4. The lattice Hamiltonian is constructed by creation and annihilation operators, $c_{\mathbf{r}}, c_{\mathbf{r}}^{\dagger}$. Due to the gauge these are two-state spinors, at different lattice sites. In the convention of [4, 9] they are spaced by a lattice constant of 1, and a hopping factor of $t$, with a phase between them explicitly written as

$$H = -t \sum_{\mathbf{r}, \hat{\mathbf{j}}} c_{\mathbf{r}+\hat{\mathbf{j}}}^{\dagger} e^{i\theta_{\hat{\mathbf{j}}}} c_{\mathbf{r}} + h.c., \tag{1.3}$$

with the phase between two sites is the path integral,

$$\theta_{\hat{\mathbf{j}}}(\mathbf{r}) = \int_{\mathbf{r}}^{\mathbf{r}+\hat{\mathbf{j}}} A_{AB,\hat{\mathbf{j}}}(r) dr. \tag{1.4}$$

We will not go into detail about the calculations to compute the Weyl Hamiltonian as it is not the goal of this thesis. The $\mathbf{r}$ is broken up into sums over x,y and z postions with a lattice constant of 1. The creation/annihilation operators' Fourier counterparts are used to achieve the Hamiltonian in momentum space $\mathbf{k}(k_x, k_y, k_z)$ [9]. The Brillioun Zone (BZ) in this scheme is split into 4 squares each of area $\pi \times \pi$ where each square are coupled to the square in the opposite corner, effectively introducing a new degree of freedom; a pseudo-spin $\tau_i$. The sum can be simplified for all the directions, yielding,

$$H(\mathbf{k}) = -2t\tau_x \cos k_x + 2t\tau_y \cos k_y - 2t\tau_z \cos k_z. \tag{1.5}$$

To realize the Hamiltonian in Eq. 1.3 in 2 dimension (2D), Raman lasers are employed. To achieve a 4 double-Weyl Hamiltonian a non-Abelian gauge, constructed by Pauli matrices $\sigma_i$, is introduced to the gauge in Eq. 1.2,

$$\mathbf{A}(y, z) = \mathbf{A}_{AB} + q \begin{pmatrix} \sigma_x \\ \sigma_y \\ 0 \end{pmatrix}, \tag{1.6}$$

which constitute a Hamiltonian of the form,

$$H(\mathbf{k}, q) = t \sum_{\mathbf{r}, S, S'} c_{\mathbf{r}, S}^{\dagger} U_{\hat{\mathbf{j}}, S, S'} c_{\mathbf{r}+\hat{\mathbf{j}}, S'} + H.C. \quad U_{\hat{\mathbf{j}}, S, S'} = \mathcal{P} e^{i \int_{\mathbf{r}}^{\mathbf{r}+\hat{\mathbf{j}}} A_{\hat{\mathbf{j}}}(r) dr}. \tag{1.7}$$

The path ordering, $\mathcal{P}$, can with great succes be removed. Even with the introduction of a non-Abelian gauge potential, the gauge still commutes at each point in space with another point in space. The Hamiltonian that we aquire is,

$$U_x = e^{i\theta_x}(\cos q \mathcal{I}_{2 \times 2} + i \sin q \sigma_x) \quad U_y = e^{i\theta_y}(\cos q \mathcal{I}_{2 \times 2} + i \sin q \sigma_y)$$

$$H = 2t\Big( -\cos q \cos k_x \tau_x \otimes \mathcal{I} + \cos q \cos k_y \tau_y \otimes \mathcal{I} - \cos q \cos k_z \tau_z \otimes \mathcal{I}$$

$$+ \sin q \sin k_x \tau_x \otimes \sigma_x - \sin q \sin k_y \tau_y \otimes \sigma_y \Big). \tag{1.8}$$

**(a)** The dispersion opens a gap when $k_x \neq 0$ and without a gap for $k_x = 0$ seen when changing $k_z$

**(b)** The dispersion opens a gap when $k_x \neq 0$ and without a gap for $k_x = 0$ seen when changing $k_y$

**(c)** The dispersion opens a gap when $k_z \neq 0$ and without a gap for $k_z = 0$ seen when changing $k_x - k_y$
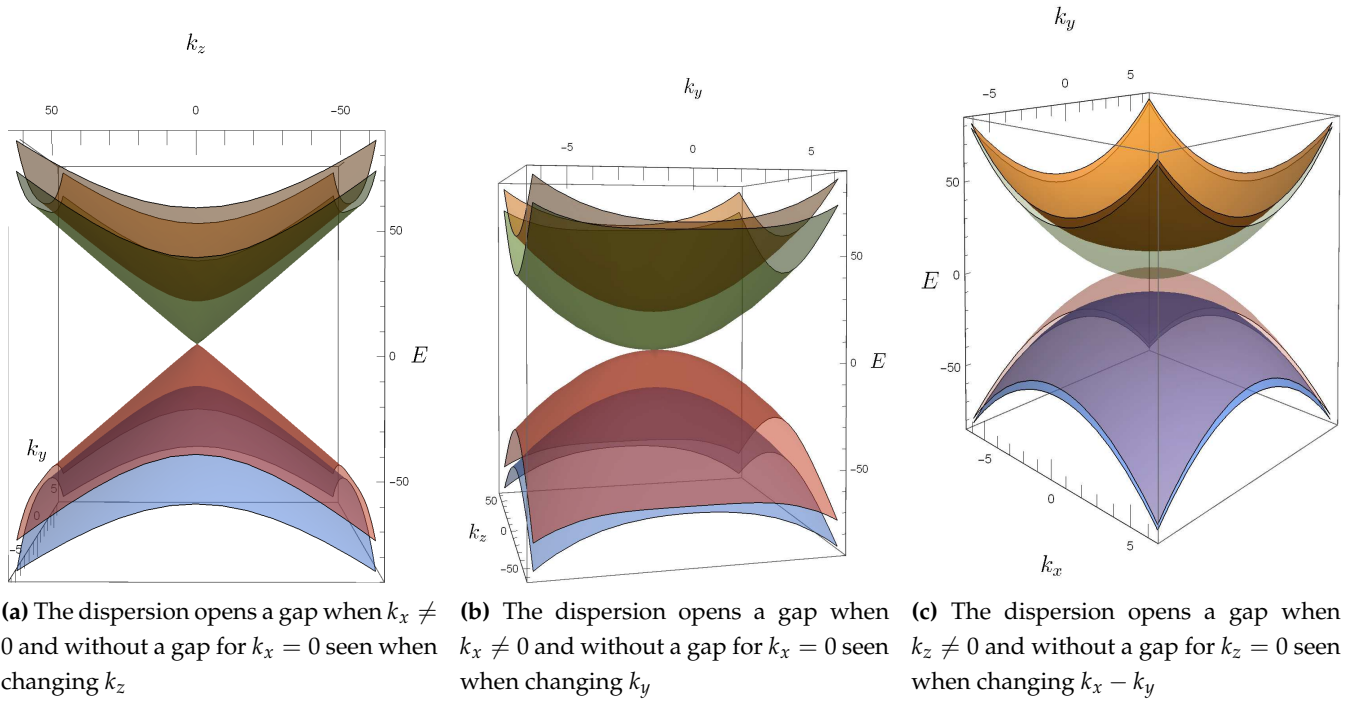
**Figure 1: Energy dispersion** of effective Hamiltonian. A reasonable guess would be that, that whether the variable under change is $k_y, k_x$ or $k_z$ will have an impact on the evolution of the system's state; if the dispersion is either quadratic or linear.

This is a 4 band Hamiltonian, but in a perturbative limit it reduces to Eq. 2.1 with the energy dispersion shown in Fig. 1. The experimental realization of the non-Abelian gauge is still an open discussion, with rare earth metals and Ytterbium being the most relevant points of interest [10, See Fig. 2]. Even the realization of the 3 dimensional (3D) Abelian gauge is not a settled matter. I have presented the Hasegawa gauge which can be realized by Raman lasers. Another way to achieve Weyl nodes is by stacking 2D sheet with Dirac cones, breaking the translational symmetry in the z-direction and then employing Raman lasers to assist hopping [11]. With other systems' Hamiltonians being realized, their topology probed and their edge states observed [12], the future of UC atom trap simulations are, however, bright.

## 2 Landau-Zener tunneling

This section will focus on deriving the non-adiabtic first order transition amplitudes of an atom subjected to a constant force of magnitude $F$. The transition for a quadratic dispersion of a double-Weyl node, as we will see, has another probabilty than that of the linear dispersion of a single Weyl node. The method has been used to calculate the transition amplitudes for an atom moving past Dirac cones [13], which have been measured experimentally [14]. As mentioned in Sec. 1.1, our case can be thought of as a 3D extension of this. A graphene sheet with Dirac cones are stacked to form line nodes, and breaking the translational invariance along the z direction forms Weyl nodes. An atom is prepared adiabatically at time $t = -\infty$ in the lower band of the effective Hamiltonian in Eq. 2.1 and a force in the direction $\hat{\mathbf{n}}$ begins to move the atom such that $\partial_t[\mathbf{k}(t)] = F\hat{\mathbf{n}}$. As it moves through momentum space (See Fig. 1), it can approach a band touching point. Displaced from these points the evolution of the states is quasi-adiabatic; and according to the adiabatic theorem there should be no transfer of particles between the bands, except at the bandtouching point. I will reference the theorem several times through out the thesis, so we define it as Born and Fock writes it:

> *A physical system remains in its instantaneous eigenstate if a given perturbation is acting on it slowly enough and if there is a gap between the eigenvalue and the rest of the Hamiltonian's spectrum*

However, due to the finitely slow velocity, the two bands interact close to the node under the exchange of the state's amplitude: As it moves through the BZ, and the difference between the two bands shrinks, the adiabatic theorem collapses. Landau-Zener transitions are a very general concepts and have been employed in many different areas. Its description were originally used to describe atomic collisions [15], but as we will show the generality and simplicity of coupling two-level system non-adiabatically is a great strength, and proves its universality.

## 2.1 The Hamiltonian; the states and energies

With the realization of 4 double-Weyl nodes in a cubic lattice structure in the UC atom trap, the problem is further simplified for low energy atoms, close to the nodes, by the perturbative approximation of a two level system. The effective Hamiltonian that this thesis will center around is,

$$\mathcal{H} = \begin{pmatrix} k_z & k_-^2 \\ k_+^2 & -k_z \end{pmatrix} = \mathbf{S}(\mathbf{k}(t)) \cdot \sigma, \tag{2.1}$$

where $\mathbf{S}(\mathbf{k}(t))$ is a Bloch vector (See Eq. 2.3). The momenta of this toy Hamiltonian should be corrected by their effective velocities, $\alpha, \beta$ and $v_z$, as menitioned in [13]. We will discuss the dimensions of the Hamiltonian in Sec. 2.2. The Hamiltonian has, in this continuum limit, an O(2) symmetry about the $z$-axis. It is written in terms of the Pauli vector and a Bloch vector, with $k_\pm = k_x \pm ik_y$. The vector $\mathbf{k}(t)$, will in this thesis always change with a force of linear time dependency. For simplicity we retract this explicit dependency, so $\mathbf{k}(t) \equiv \mathbf{k}$. As the Hamiltonian is simply the product between the vector $\mathbf{S}(\mathbf{k})$ and the Pauli vector, the states and energies are characterized by a Bloch sphere notation (See Appendix 8.C). We introduce a gauge transformation of $e^{-i\phi_S(\mathbf{k})/2}$, with $\phi_S$ being the azimuthal angle of the Bloch vector. We can also conclude that shifting the polar angle of S, $\theta_S$, by $\pi/2$ two states, an upper $\psi_+$ and lower $\psi_-$, which is still orthogonal and eigenstates to the Hamiltonian with the correct energies, $E_\pm$, can be separated,

$$|\psi_-(\mathbf{k})\rangle = \begin{pmatrix} \sin(\theta_S(\mathbf{k})/2)e^{-i\phi_S(\mathbf{k})/2} \\ -\cos(\theta_S(\mathbf{k})/2)e^{i\phi_S(\mathbf{k})/2} \end{pmatrix}, \quad |\psi_+(\mathbf{k})\rangle = \begin{pmatrix} \cos(\theta_S(\mathbf{k})/2)e^{-i\phi_S(\mathbf{k})/2} \\ \sin(\theta_S(\mathbf{k})/2)e^{i\phi_S(\mathbf{k})/2} \end{pmatrix},$$

$$E_\pm(\mathbf{k}) = \pm|\mathbf{S}(\mathbf{k})| = \pm\sqrt{k_z^2 + (k_x^2 + k_y^2)^2}, \tag{2.2}$$

with the Cartesian and spherical coordinates of the Bloch vector,

$$\mathbf{S}(\mathbf{k}) \overset{\text{cart.}}{=} \begin{pmatrix} S_x(\mathbf{k}) \\ S_y(\mathbf{k}) \\ S_z(\mathbf{k}) \end{pmatrix} = \begin{pmatrix} (k_x^2 - k_y^2) \\ 2k_xk_y \\ k_z \end{pmatrix} \overset{\text{sphe.}}{=} \begin{pmatrix} |S|(\mathbf{k}) \\ \theta_S(\mathbf{k}) \\ \phi_S(\mathbf{k}) \end{pmatrix} = \begin{pmatrix} \sqrt{S_x^2 + S_y^2 + S_z^2} \\ \arccos\dfrac{S_z}{\sqrt{S_x^2 + S_y^2 + S_z^2}} \\ \arctan\dfrac{S_y}{S_x} \end{pmatrix} = \begin{pmatrix} E_+(\mathbf{k}) \\ \arccos\dfrac{k_z}{E_+(\mathbf{k})} \\ \arctan\dfrac{2k_xk_y}{k_x^2 - k_y^2} \end{pmatrix}. \tag{2.3}$$

The gauge transformation will be helpful to obtain an easy to use timedependency of the states. The instantaneous eigenstates of the Hamiltonian correspond to an upper and a lower band, $E_\pm(\mathbf{k})$. Due to the linearity of the force, instantaneous eigenstates are a decent basis; the Hamiltonian is diagonalized with regards to the force, and therefore time, as the parameter (See Eq. 2.4). The bands touch in the Weyl nodes, where the adiabatic theorem, breaks down, as the atom's neighbourhood at such a point will contain the non-adiabatic band touching point. If an atom is loaded in the lower band, adiabaticly, there

is no transition probability discplaced from these nodes. However, close to the crossing, the energy bands exhibit a avoided-touching appearence where a non-adiabatic Landau-Zener (LZ) tunneling event can take place. We will throughout this thesis use a parameter $\mathbf{k}_0$ to displace the atom from the band touching point, so when the atom moves through the BZ it moves past the point; close to it, but not into it. This thesis researches 3 cases (See Table 1) of displacement from the bandtouching point. In each case, the atom starts so far from the bandtouching point that the adiabatic theorem holds, even for finitely slow velocities. We then move the atom with a force F past the bandtouching point, with a parameter $k_0$, that tunes how far from the point the atom is when it is at its closest. The method of Landau and Zener is that when we obtain the amplitude at $t = \infty$, the explicit time dependency is not needed [16].

|  | Moving in $k_z$ | Moving in $k_x$ | Moving in $k_x$ |
|---|---|---|---|
| Displacement: | $k_x$-$k_y$-plane | $k_z$ | $k_y$ |
| S-parameters | $\partial_t \theta_S = 0$ | $\partial_t \phi_S = 0$ | $\partial_t \phi_S = 0$ |

**Table 1: The three cases**, this thesis will research to obtain the probabability of tunneling to the upper state. The three cases of displacement from the bandtouching point and the Bloch vector's time dependency in each cases. The length of the vector is always time dependent, but as we will see, the length of the Bloch vector will not play into the time-dependent perturbation theory that we use in this thesis.

The general time dependency of the amplitudes, $A_\pm(t)$, of the two adiabatic states satisfy the time-dependent Schrödinger equation. Any instantaneous wavefunction, $|\Psi(t)\rangle$ can be written as a linear combination of the instantaneous eigenstates, $|\psi(t)_\pm\rangle$, the time-dependent amplitudes, $A_\pm(t)$ and a dynamical phase [17],

$$|\Psi(t)\rangle = A_+(t)e^{i\int^t dt' E_+(t')}|\psi_+(t)\rangle + A_-(t)e^{i\int^t dt' E_-(t')}|\psi_-(t)\rangle. \tag{2.4}$$

The Schrödinger equation can be reduced to,

$$\partial_t A_\pm(t) + A_\pm(t)\langle\psi_\pm(t)|\partial_t\psi_\pm(t)\rangle = -\langle\psi_\pm(t)|\partial_t\psi_\mp(t)\rangle A_\mp(t)e^{\pm 2i\int^t dt' E_+(\mathbf{k}(t'))}, \tag{2.5}$$

due to the fact $E_+(\mathbf{k}(t)) = -E_-(\mathbf{k}(t))$. Furthermore, for all of the cases $\langle\psi_\pm(t)|\partial_t\psi_\pm(t)\rangle = 0$. This is due to the fact that $|\partial_t\psi_\pm(t)\rangle \propto |\psi_\mp(t)\rangle$ with $\langle\psi_\alpha|\psi_\beta\rangle = \delta_{\alpha\beta}$. We then obtain the differential equation,

$$\partial_t A_\pm(t) = -\langle\psi_\pm(t)|\partial_t\psi_\mp(t)\rangle A_\mp(t)e^{\pm 2i\int^t dt' E_+(\mathbf{k}(t'))}, \tag{2.6}$$

where $\langle\psi_\pm(t)|\partial_t\psi_\mp(t)\rangle$ corresponds to the force coupling the adiabatic eigenstates of the Hamiltonian. The adiabatic basis can relatively easily be held up against that measured in experiments [18]. After the atoms have evolved through the BZ, the experimenter can take a snapshot of the atom cloud and the state will be frozen in the linear combination of the instantaneous Hamiltonian. The differential equations of Eq. 2.6 are solved by time-dependent perturbation theory (TDPT). For each case the Hamiltonian, the eigenstate and the energies of interest are presented. After the calculations we will quickly conclude and present the results.

### 2.1.1 Movement in $k_z$, displacement in the $k_x - k_y$ plane

The first case is akin to that of the regular LZ problem in 3D [15]. It will be a method to compare the results found in the next two cases, which are arguably more complicated, with the same method used on a problem that is well documented. The force is in the $k_z$ direction and we have a displacement from the node in the $k_x - k_y$ plane. Due to the O(2) symmetry in the $k_x - k_y$ plane, the dispalacement can be is

defined by cylindrical coordinates $\mathbf{k}_\Gamma = (k_{0,\Gamma}, \theta_\Gamma, k_z)$, instead of taking specific coordinate. The Hamiltonian is,

$$\mathcal{H} = \begin{pmatrix} Ft & \Gamma \\ \Gamma^* & -Ft \end{pmatrix} = k_{0,\Gamma}^2 \cos 2\theta_\Gamma \sigma_x + k_{0,\Gamma}^2 \sin 2\theta_\Gamma \sigma_y + Ft\sigma_z, \tag{2.7}$$

with $\Gamma = k_{0,\Gamma}^2 e^{-2i\theta_\Gamma}$. The time dependency, which can be obtained by a simple change of the derivative parameter, of the states in Eq. 2.2 are only dependent in the $\theta_S$ parameter of Eq. 2.3,

$$|\partial_t \psi_\pm(t)\rangle = \mp \frac{\partial_t \theta_S(t)}{2}|\psi_\mp(t)\rangle \qquad\qquad E_\pm(t) = \pm F\sqrt{t^2 + k_{0,\Gamma}^4/F^2}, \tag{2.8}$$

and the amplitudes then satisfy Eq. 2.6. The time derivative of $\theta_S(t)$ is given by $\partial_t \theta_S(t) = -\frac{Fk_{0,\Gamma}^2}{E_+(t)^2}$. This is used to set up the differential equation in Eq. 2.6. The integral we want to obtain for $A_+(\infty)$ is,

$$A_+(\infty) = -\int_{-\infty}^{\infty} dt \frac{Fk_{0,\Gamma}^2}{2E_+(t)^2} \cdot e^{2i\int^t dt' E_+(t')}. \tag{2.9}$$

This integral has two poles in the Argand plane, $\pm \frac{ik_{0,\Gamma}}{F}$. The exponential of the $dt'$-integral can be moved out of the $dt$-integral, and the phase of Eq. 2.9 can then be evaluated in the pole enclosed in the contour that closes the integral of $A_+(t)$. Naively one could think that it is the application of Cauchy's theorem that allows this. However, we identify that the funtion is not single valued around the time pole; rotating $2\pi$ around the pole will not yield the same functional value, and therefore Cauchy's theorem is not applicable (See discussion in Appendix 8.A and proof by [19]). To solve the exponential integral we use a trigonometric substitution with a new intragtion variable, $\tilde{\theta}$, so that $t = \tan(\tilde{\theta})k_0^2/F$. The integral evaluated at the upper half plane pole yields,

$$F\int_0^{t_0} dt \sqrt{t^2 + k_{0,\Gamma}^4/F^2} = \frac{k_{0,\Gamma}^4}{2F}\ln\left(\frac{F}{k_{0,\Gamma}^2}t_0\right) = \frac{ik_0^4\pi}{4F}. \tag{2.10}$$

The pole enclosed in the contour are in the upper half plane, due to $E_+ > 0$, and it is a result of the singularity in $\partial_t \theta_S$, which is $t_0 = ik_{0,\Gamma}^2/F$. The residue at this first order pole is,

$$R_{t_+} = \lim_{t \to ik_{0,\Gamma}^2/F} -\frac{k_{0,\Gamma}^2}{Ft + ik_{0,\Gamma}^2} = \frac{i}{2}, \tag{2.11}$$

which leaves us the probability,

$$P_+(\infty) = |A_+(\infty)|^2 = \frac{\pi^2}{4}e^{-\frac{\pi k_{0,\Gamma}^4}{2F}}. \tag{2.12}$$

This result is expected from the classical LZ problem[15, 20], with a linear adiabacity parameter $\delta = k_{0,\Gamma}^4/4F$. We can also write it without the prefactor, that stems from it being a first order perturbation theory [13].

$$P_+(\infty) = |A_+(\infty)|^2 = e^{-\frac{\pi k_{0,\Gamma}^4}{2F}}. \tag{2.13}$$

### 2.1.2 Movement in $k_x$, displacement in $k_z$

Moving in the $k_x$ direction with a displacement in $k_y$ the Hamiltonian is given by,

$$\mathcal{H} = \begin{pmatrix} k_z & F^2t^2 \\ F^2t^2 & k_z \end{pmatrix} = k_z\sigma_z + F^2t^2\sigma_x, \tag{2.14}$$

with the two states and energies

$$|\psi_+\rangle = \begin{pmatrix} \cos(\theta_S/2) \\ \sin(\theta_S/2) \end{pmatrix}, \quad |\psi_-\rangle = \begin{pmatrix} \sin(\theta_S/2) \\ -\cos(\theta_S/2) \end{pmatrix} \qquad E_\pm = \pm\sqrt{k_z^2 + (Ft)^4}. \tag{2.15}$$

This is the case that [13, 21] discuss. A sliver of our double-Weyl momentum space is equal to their case of two displaced Dirac cones with a quadratic dispersion in one direction. The major difference between this case and the previous of the regular/linear LZ problem is that the squareroot in the time integral of the energy is a squareroot of a hyperpolynomial. We will discuss this later in the section and Appendix 8.E. Now we define the differential equation (Eq. 2.6) to be solved. The following couplings are calculated,

$$-\langle\psi_+|\partial_t\psi_-\rangle = \langle\psi_-|\partial_t\psi_+\rangle = \frac{\partial_t\theta_S}{2},$$

$$\partial_t\theta_S = \frac{2k_{0,z}F^4t^3}{\left(F^4t^4 + k_{0,z}^2\right)\sqrt{F^4t^4}} = \frac{2k_{0,z}F^2t}{\left(E_+\right)^2}. \tag{2.16}$$

We are left with an equation for the upper band amplitude, at first order with the zeroth order amplitude $A_-^{(0)}(t) = 1$,

$$\partial_t A_+(t) = -\langle\psi_+|\partial_t\psi_-\rangle A_-(t)e^{2i\int^t dt' E_+(t')} = \frac{\partial_t\theta_S}{2}e^{2i\int^t dt' E_+(t')}, \tag{2.17}$$

with the poles given below,

$$t_0 = \left\{ \pm e^{3i\pi/4}\frac{\sqrt{k_{0,z}}}{F}, \pm e^{i\pi/4}\frac{\sqrt{k_{0,z}}}{F} \right\}. \tag{2.18}$$

Integration in the upper plane closes the integral. The fact that there are two poles in each half plane, will create oscillations as the two interfere [13]. Now we introduce a Taylor expansion of the energy integral. Due to the integral of the squareroot of a quaternic polynomial in the exponent, the time evolution found with Eq. 2.6 has an exponential integral, which arises from the dynamical phases, where at one of the poles it is equal to an incomplete elliptical function of first kind, which this thesis will avoid to delve too far into (See Appendix 8.E, where it is solved). Instead the energy is expanded. This still leaves the correct k:F ratio only with a different factor in front of it. In Sec. 2.3 we expand in another variable than what we integrate over. This is achieved by making it slightly anisotropic, and expanding in the anisotropy. Instead of solving a O(2) symmetric Hamiltonian, a $C_4$ symmetric Hamiltonian is instead solved. For now we will expand in time around the complex pole, with $\delta t$ being the small step away from the pole,

$$E_+(\delta t) \simeq \sqrt{4F^4t_0^3\delta t} \Rightarrow \int_0^{t_0} d(\delta t)E_+(\delta t) = \frac{2}{3F}k_{0,z}^{3/2}e^{3i\pi/4} \quad \vee \quad \frac{2}{3F}k_{0,z}^{3/2}e^{9i\pi/4}, \tag{2.19}$$

for respectively $t_1 = \frac{\sqrt{k_{0,z}}}{F}e^{i\pi/4}$ and $t_2 = \frac{\sqrt{k_{0,z}}}{F}e^{3i\pi/4}$. Calculating the residue of each pole yield

$$R_{\sqrt{k}e^{i\pi/4}/F}(\partial_t\theta_S) = -\frac{i}{2}, \qquad R_{\sqrt{k}e^{3i\pi/4}/F}(\partial_t\theta_S) = \frac{i}{2}. \tag{2.20}$$

We gather the result obtain a transition probability of,

$$P_+(\infty) = |A_+(\infty)|^2 = \pi^2\left( \sin\left(\frac{2\sqrt{2}}{3F}k_{0,z}^{3/2}\right)^2 \right)e^{-\frac{4\sqrt{2}}{3F}k_{0,z}^{3/2}}. \tag{2.21}$$

### 2.1.3 Movement in $k_x$, displacement in $k_y$

Moving in $k_x$ with a displacement in $k_y$ the Hamiltonian is completely off-diagonal,

$$\mathcal{H} = \begin{pmatrix} 0 & ((Ft)^2 - k_y^2) - 2ik_yFt \\ ((Ft)^2 - k_y^2) + 2ik_yFt & 0 \end{pmatrix} = ((Ft)^2 - k_y^2)\sigma_x + 2k_yFt\sigma_y. \tag{2.22}$$

In comparison with the previous two cases this case is entirely new, peculiar to a double-Weyl Hamiltonian and to my knowledge not covered before. The states and energies are given in Eq. 2.2, but in this case we

have no $k_z$ displacement. To obtain the differential equations (Eq. 2.6) for this case the coupling between the adiabatic eigenstates, when subjecting the system to a force along $k_x$, is calculated as,

$$\langle \psi_+ | \partial_t \psi_- \rangle = \langle \psi_- | \partial_t \psi_+ \rangle = \frac{\partial_t \phi_S}{2i}. \tag{2.23}$$

The time-dependency is obtained as,

$$\partial_t \phi_S = -\frac{2 \cdot k_{0,y} \cdot F}{k_{0,y}^2 + F^2 t^2} = -\frac{2 \cdot k_{0,y} \cdot F}{E_+}, \tag{2.24}$$

which implies,

$$\partial_t A_\pm(t) = -\frac{\partial_t \phi_S}{2i} A_\mp(t) e^{\pm 2i \int^t dt' E_+(t')}. \tag{2.25}$$

This equation has simple poles in $t_\pm = \pm i \frac{k_0}{F}$. The differential is treated with first order TDPT, where $A_-(-\infty) = 1$ and $A_-^{(0)}(t) = 1$, so that the coupling is small; the system is treated as if it is perturbed by a small coupling of $\partial_t \phi_S \propto F$ and $\partial_t \phi_S \neq 0$ if the path through the BZ is displaced from the node. Integrating over $t(-\infty; \infty)$, the exponential can be moved out of the integral with the assumption made by Dykhne [13, 19] (See Appendix 8.A). Another method is to integrate over the aquired phase $\phi_P = 2 \int^t dt' E_+(t')$ [13, 21, 22]. By this substitution branch cuts eminating from the poles can be avoided. Continuing with the same method results in the integral,

$$A_+(\infty) = -\frac{1}{2i} e^{2i \int^{t_+} dt' E_+(t')} \int_{-\infty}^{\infty} dt \partial_t \phi_S(t). \tag{2.26}$$

The pole of the integral that is enclosed in the contour, C, is that in the upper plane, $t_+$, yielding,

$$-\frac{1}{2i} \int_{-\infty}^{\infty} dt \partial_t \phi_S(t) = -\frac{1}{2i} \oint_C dt' \frac{-2k_{0,y}F}{E_+(t)} = \frac{-2\pi i}{2i} \text{Res}_{t_+} = \pi i. \tag{2.27}$$

The exponential integral evaluated at the pole is

$$\phi_P(t_+) = 2i \int^{t_+} E_+(t) = i \frac{4k_{0,y}}{3F}. \tag{2.28}$$

The probability to find the particle in the upper state is then,

$$P_+(\infty) = |A_+(\infty)|^2 = \pi^2 e^{-\frac{8k_{0,y}^3}{3F}}. \tag{2.29}$$

## 2.2 Conclusion on Landau-Zener transitions, first order time-dependent pertubation theory and dimension analysis

Recap of this section is a brief summarization of the 3 cases in Table 1. There is a prefactor error in all cases, which arises from the fact that the calculations are only first order [13]. To calculate the amplitude we have split the integral of the differential equation of Eq. 2.6 in two products. One is the phase that must be evaluated from 0 to the pole in question, and the other is the residue of the pole. If we have two poles it is the sum of this methods for each pole. There is also the problem that for now the Hamiltonian has been dimensionless. To correct this we introduce a velocity $v_z$ and a relative velocity $\beta$ is, which yields the correct Hamiltonian,

$$\mathcal{H} = \begin{pmatrix} k_z & k_-^2 \\ k_+^2 & -k_z \end{pmatrix} \Rightarrow \begin{pmatrix} v_z k_z & \beta k_-^2 \\ \beta k_+^2 & -v_z k_z \end{pmatrix}. \tag{2.30}$$

In this thesis $\hbar = 1$, so $J = \frac{1}{s}$. The principle is to find the dimensions of $\beta$ and $v_z$, by first looking at the energy and then conclude that the exponential must be dimensionless. From analysis of the energy we find that,

$$[E] = \left[ \sqrt{v_z^2 k_z^2 + \beta^2 (k_x^2 + k_y^2)^2} \right] = J = \frac{1}{s}, \tag{2.31}$$

8

$$[\beta] = \frac{1}{N^2 s^3} = \frac{s}{kg^2 m^2} \quad , \quad [v_z] = \frac{1}{N \cdot s^2} = \frac{1}{kg \cdot m}. \tag{2.32}$$

| | Moving in $k_z$ displacement $k_x k_y$-plane | Moving in $k_x$ displacement $k_z$ | Moving in $k_x$ displacement in $k_y$ |
|---|---|---|---|
| $P_{LZ}$: | $e^{-\frac{\pi k_{0,\Gamma}^4}{2F}}$ | $\pi^2 \sin^2\left(\frac{2\sqrt{2}}{3F}k_{0,z}^{3/2}\right)e^{-\frac{4\sqrt{2}}{3F}k_{0,z}^{3/2}}$ | $\pi^2 e^{-\frac{8k_{0,y}^3}{3F}}$ |
| Approximation? | Exact | First order + Taylor | First order + O(2) symmetric |
| Exponent | $\dfrac{k_{0,\Gamma}^4}{F}$ | $\dfrac{k_{0,z}^{3/2}}{F}$ | $\dfrac{k_{0,y}^3}{F}$ |
| Dimensionless if | $\dfrac{\beta^2}{v_z}\dfrac{k_{0,\Gamma}^4}{2F}$ | $\dfrac{v_z^{3/2}}{\sqrt{\beta}}\dfrac{k_{0,z}^{3/2}}{3F}$ | $\beta\dfrac{k_{0,y}^3}{3F}$ |

**Table 2:** The three cases' probability of a Landau-Zener tunneling $P_{LZ}$, how the exponential integral is solved and the introduction of $v_z$ and $\beta$. When moving in $k_z$ I have written the case of summing all orders in the perturbation theory. This removes the prefactor. The other two cases are first order TDPT

## 2.3 Breaking the O(2) symmetry of the system

The Hamiltonian of Eq. 2.1 is a special O(2) symmetric case of a more general, $C_4$ symmetric Hamiltonian, which is written with its dimensions $\alpha, \beta$ and $v_z$,

$$\mathcal{H} = \begin{pmatrix} v_z k_z & \alpha K_+^2 + \beta K_-^2 \\ \alpha K_-^2 + \beta K_+^2 & -k_z \end{pmatrix} = k_z \sigma_z + (\beta - \alpha)(2k_x k_y)\sigma_y + (\alpha + \beta)(k_x^2 - k_y^2)\sigma_x. \tag{2.33}$$

The differential is still defined by Eq. 2.6 with a force driving the atom, and coupling the adiabatic eigenstates of Eq. 2.2. The O(2) case is $\alpha = 0$. The energy is corrected to

$$E_+ = \sqrt{v_z^2 k_z^2 + \left(\alpha + \beta\right)^2 \left(k_x^2 - k_y^2\right)^2 + \left(\beta - \alpha\right)^2 \left(2k_x k_y\right)^2}. \tag{2.34}$$

The coupling between the two eigenstates of Eq. 2.2 will still be either

$$\langle \psi_+ | \partial_t \psi_- \rangle = -\frac{\partial_t \theta_S}{2} \vee \frac{\partial_t \phi_S}{2i}, \tag{2.35}$$

depending on the case, as no new explicit time dependency is introduced. However, it alters the time dependency of the Bloch vector parameter, where now,

$$\phi_S = \tan^{-1}\left(\frac{(\beta - \alpha)2k_x k_y}{(\alpha + \beta)(k_x^2 - k_y^2)}\right),$$

$$\theta_S = \cos^{-1}\left(\frac{v_z k_z}{\sqrt{v_z^2 k_z^2 + \left(\alpha + \beta\right)^2 \left(k_x^2 - k_y^2\right)^2 + \left(\beta - \alpha\right)^2 \left(2k_x k_y\right)^2}}\right), \tag{2.36}$$

and as such this equation introduce a correction to the wavefunction of Eq. 2.4. It also alters the poles in the complex time plane of Eq. 2.35. For the case of moving in $k_x$ and having a displacement in $k_y$ there are 4 poles,

$$t_0 = \pm\frac{k_{0,y}}{\xi F} \cdot \sqrt{\xi^2 \pm 2\sqrt{-\xi^2 + 1} - 2} \quad , \quad \xi = \frac{\beta - \alpha}{\beta + \alpha}. \tag{2.37}$$

In the case of moving in $k_x$ and with a displacement in $k_z$ there are also 4 poles.

$$t_0 = \sqrt{\frac{v_z k_z}{\alpha + \beta} \frac{1}{F}} \cdot \eta, \quad \eta = \left\{ \pm(-1)^{1/4}, \pm(-1)^{3/4} \right\}, \tag{2.38}$$

This yields the same poles, when we remove the anisotropy. Due to the anisotropy, to solve the integrals, we obtain a correction to the energy and time dependency. To obtain an approximate solution of the phase integral in Eq. 2.2, we expand the energy, to obtain an integral, where the energy for the three cases is expanded in a small anisotropy ($\alpha \to 0$), which is actually so small that even the displacement from the isotropic case $\delta\alpha \to 0$. As such the expansions yields, for the case of $k_y = 0$

$$
\begin{aligned}
E_+ &\simeq \sqrt{v_z^2 k_z^2 + \beta^2 k_x(t)^4 + 2\beta k_x(t)^4 \delta\alpha} \\
&\simeq \sqrt{v_z^2 k_z^2 + \beta^2 k_x(t)^4} \left( 1 + \frac{\beta^2 k_x(t)^4}{v_z^2 k_z^2 + \beta^2 k_x(t)^4} \delta\alpha \right),
\end{aligned}
\tag{2.39}
$$

and for the case of $k_z = 0$

$$
\begin{aligned}
E_+(t) &\simeq \sqrt{\beta^2(k_x(t)^2 + k_y^2)^2 + 2\beta((k_x(t)^2 - k_y^2)^2 - (2k_x(t)k_y)^2)\delta\alpha} \\
&\simeq \beta(k_x(t)^2 + k_y^2) + \frac{(k_x(t)^2 - k_y^2)^2 - (2k_x(t)k_y)^2}{k_x(t)^2 + k_y^2} \delta\alpha,
\end{aligned}
\tag{2.40}
$$

with $k_x(t) = F \cdot t$. Naturally we obtain a correction term that is linear in the anisotropy, as we only go to first order. Notice that in both cases when the squareroot is raised, the postive solution is chosen to give the upper band energy. These new functions are analytic except in a finite amount of poles. For the case of $k_z = 0$ the correction as a function of $\delta\alpha$ in the phase integral is

$$\int_0^{t_0} \frac{(F^2 t^2 - k_{0,y}^2)^2 - (2Ftk_{0,y})^2}{F^2 t^2 + k_{0,y}} \delta\alpha = \left[ t_0 \left( \frac{1}{3} F^2 t_0^2 - k_{0,y} - 6k_{0,y}^2 \right) + \frac{1}{F} \left( k_{0,y}^{3/2} (1 + 6k_{0,y} + k_{0,y}^2) \tan^{-1} \left( \frac{Ft_0}{k_{0,y}} \right) \right) \right] \delta\alpha. \tag{2.41}$$

In the case of $k_y = 0$, hypergeometric functions, $_pF_q[\mathbf{a}; \mathbf{b}; z]$ are obtained. In this thesis we will not go into details about these corrections, but simply boint out that they exist and should be considered.

## 3  Stückelberg oscillations

Stückelberg oscillations occur when the particle moves past two avoided band-touching point (See Fig. 2). As the amplitudes of the state move in the upper or lower band the accumulated phase differ (See Eq. 2.4)[18, 23, 24]. This is the method of Stückelberg interferometry. The interferometer in this case is not a object/lab equipment that is situated in real space. Instead, the two avoided band-touching points in momentum space, where a non-adiabtic transition can take place, can to some extent be thought of as beam-splitters, and the adiabatic evolution between to nodes causes interference. In our case, the general Hamiltonian of Eq. 2.33 allow for two the Weyl points to have different topological charge of $-2$ and $+2$, with repectively the two Hamiltonians, that approximate the dispersion in the vicinity of the nodes.

$$\mathcal{H}_\beta^- = \begin{pmatrix} k_z & \beta k_-^2 \\ \beta k_+^2 & -k_z \end{pmatrix} \quad , \quad \mathcal{H}_\alpha^+ = \begin{pmatrix} k_z & \alpha k_+^2 \\ \alpha k_-^2 & -k_z \end{pmatrix}. \tag{3.1}$$

In Eq. 3.1 the plus and minus of the Hamiltonian refers to the polarity of the node. This charge will also be calculated in Sec. 4. In momentum space the nodes correspond to magnetic monopoles, and depending on the sign, we can label them as either a source(+) or a sink(-). $\alpha, \beta$ is the prefactor on the off-diagonal,
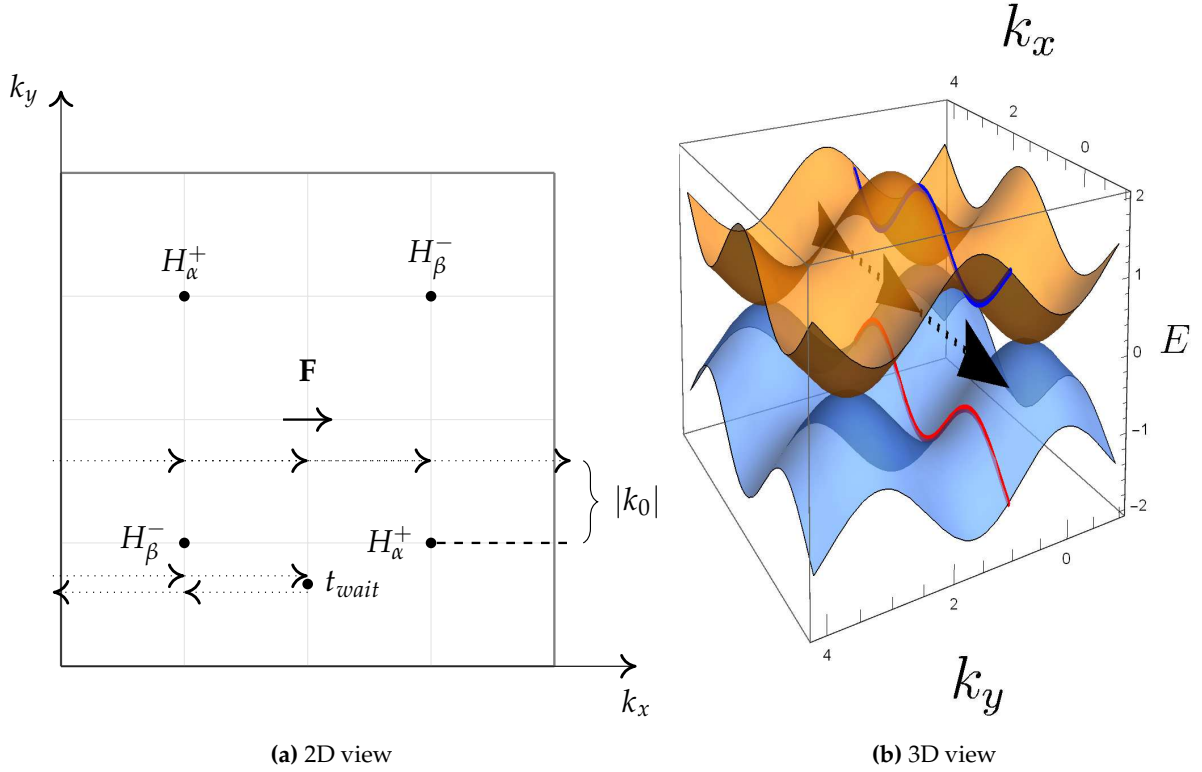
**(a)** 2D view

**(b)** 3D view

**Figure 2: The path through the Brillouin Zone:** The red and blue lines demonstrate how a sliver of the BZ's energy dispersion appear, when traveling in the dotted arrowed path driven by the force **F**. a) The $1^{st}$ BZ in 2D, which is drawn as the black square, with 4 band-touching nodes. In the vicinity of these, The Hamiltonians are effectively those of Eq. 3.1. The displacement from the nodes is as always described by some $|k_0|$. The lowest path is the case of Sec. 3.1 and the upper path is that of Sec. 3 b) show the dispersion of the effective lattice Hamiltonian in 3D in Eq. 1.3 that we will cover in Sec. 4.2. The force and displacement is given by the black dotted arrow. The state will either evolve in the upper band (blue line) or lower band (red line)

and while we will keep it in the notation, for computing probabilities we will set $\alpha = \beta = 1$, which in this simple lattice model is a reasonable assumption. We still set $v_z \equiv 1$. The two Hamiltonians can be related by:

$$\mathcal{H}_\beta^+(k_y) = \mathcal{H}_\beta^-(-k_y) \quad \vee \quad \mathcal{H}_\beta^+ = \left(\mathcal{H}_\beta^-\right)^*. \tag{3.2}$$

The movement of the state through the $1^{st}$ BZ can be seperated into 4 matrices [25], which we will now go through:

$$M_{tot} = M_{dyn}^{(-,+)} M_{LZ,\alpha}^+ M_{dyn}^{(+,-)} M_{LZ,\beta}^- \tag{3.3}$$

The total matrix is the result of an LZ tunneling event at $\mathcal{H}_\beta$, the dynamical phase aquired between $\mathcal{H}_\beta$ and $\mathcal{H}_\alpha$, an avoided band touching with a second tunneling event and a new, not necessarily the same, dynamical phase, to return to the starting momentum (See Fig. 2). The LZ matrix is written as [13, 25, 26]:

$$M_{LZ}^\pm = \begin{pmatrix} \sqrt{P_{LZ}^\pm - 1} e^{-i(\phi_{St}^\pm - \pi/2)} & -\sqrt{P_{LZ}^\pm} \\ \sqrt{P_{LZ}^\pm} & \sqrt{P_{LZ}^\pm - 1} e^{i(\phi_{St}^\pm - \pi/2)} \end{pmatrix}, \tag{3.4}$$

where $P_{LZ}^\pm$ is the LZ transtion probability at a source or sink. I might add that the matrix has been found with method of [26, Appendix A], that computes it for a linear dispersion. Though it is out of the scope of this this to find it for a quadratic dispersion, in my academic analysis [27, Sec. C] and preliminary

11

theoretical analysis of the differential equations (Eq. 2.6), I have no reason to doubt its generality for the hyperpolynomial dispersions. I have presented the problem in Appendix 8.D. The Stoke phase, $\phi_{St}$, is given by [13, 21] (See Appendix 8.D)

$$\phi_{St} = \frac{\pi}{4} + \delta(\ln \delta - 1) + \Gamma(1 - i\delta), \tag{3.5}$$

where the linear adiabatic parameter, $\delta$, is defined by the LZ probability[21], $P_{LZ} \propto e^{-2\pi\delta}$. In this thesis we will leave the Stoke phase as a parameter. $\Gamma(x)$ is the Gamma function. The Hamiltonian at these poles can be related by the sign $k_y$ (Eq. 3.2). This have to be accounted for when changing the sign of $k_y$, and calculating the new probability of transition,

$$M_{dyn}^{(\pm,\mp)} = \begin{pmatrix} e^{-i\Phi_{dyn}^{(\pm,\mp)}} & 0 \\ 0 & e^{i\Phi_{dyn}^{(\pm,\mp)}} \end{pmatrix} \quad , \quad \Phi_{dyn}^{(\pm,\mp)} = \frac{1}{F} \int_{k^\mp}^{k^\pm} E_+(k)dk. \tag{3.6}$$

The dynamical matrix is a function of the phase integral from seperation of the source (denoted with a plus) and sink (denoted with a minus), $|k^\pm - k^\mp|$. It has to be noted that the relative velocity $\alpha, \beta$ also has to be accounted for. The probability to be in the upper band after a full path through the BZ, $T_{BZ}$, can be calculated from the matrix Eq. 3.3:

$$\begin{pmatrix} A_+(T_{BZ}) \\ A_-(T_{BZ}) \end{pmatrix} = M_{tot} \begin{pmatrix} 0 \\ 1 \end{pmatrix}$$

$$A_+ = -e^{-i\Phi_{dyn}^{(-,+)}}\sqrt{1 - P_{LZ,\alpha}^+}\, e^{-i(\phi_{st,\beta}^- - \pi/2)} e^{-i\Phi_{dyn}^{(+,-)}}\sqrt{P_{LZ,\beta}^-} - e^{-i\Phi_{dyn}^{(-,+)}}\sqrt{P_{LZ,\alpha}^+}\, e^{i\Phi_{dyn}^{(+,-)}}\sqrt{1 - P_{LZ,\beta}^-}\, e^{i(\phi_{st,\alpha}^+ - \pi/2)}$$

$$= -\sqrt{P_{LZ,\alpha}^+ P_{LZ,\beta}^-} \cdot e^{-i(\Phi_{dyn}^{(-,+)} - \Phi_{dyn}^{(+,-)})} \left( e^{-i(\phi_{st,\beta}^- - \pi/2 - 2\Phi_{dyn}^{(+,-)})}\sqrt{(P_{LZ,\alpha}^+)^{-1} - 1} + e^{i(\phi_{st,\alpha}^+ - \pi/2)}\sqrt{(P_{LZ,\beta}^-)^{-1} - 1} \right), \tag{3.7}$$

where $\Phi_{dyn}^{(+,-)}$ corresponds to moving from the sink to the source, which is the positions of the avoided bandtouching point for $\mathcal{H}_\beta^- / \mathcal{H}_\alpha^+$. The probability is then

$$P_+(T) = P_{LZ,\alpha}^+ P_{LZ,\beta}^- \left| \left( e^{-i(\phi_{st,\beta}^- - \pi/2 - 2\Phi_{dyn}^{(+,-)})}\sqrt{(P_{LZ,\alpha}^+)^{-1} - 1} + e^{i(\phi_{st,\alpha}^+ - \pi/2)}\sqrt{(P_{LZ,\beta}^-)^{-1} - 1} \right) \right|^2$$

$$= P_{LZ,\alpha}^+ P_{LZ,\beta}^- \left( (P_{LZ,\beta}^-)^{-1} + (P_{LZ,\alpha}^+)^{-1} - 2 \right.$$

$$\left. + 2\sqrt{(P_{LZ,\alpha}^+)^{-1} - 1) \cdot ((P_{LZ,\beta}^-)^{-1} - 1)} \cos(\phi_{st,\alpha}^+ + \phi_{st,\beta}^- + 2\Phi_{dyn}^{(+,-)}) \right). \tag{3.8}$$

Eq. 3.8 is a general Stückelberg probability for the case of the two different Hamiltonians in Eq. 3.1. We will simplify by setting $\alpha = \beta$, and Eq. 3.2 relates the two Hamiltonian with $\mathcal{H}^+(k_y) = \mathcal{H}^-(-k_y)$. We then remind ourselves that close to node the Hamiltonian, in the continuum limit, is O(2) symmetric about the z-axis. Rotating by $\pi$, $k_y \to -k_y$, will not influence the probability. This is the symmetry argument for,

$$P_{LZ}^+(k_{0,i}, F) = P_{LZ}^-(-k_{0,i}, F). \tag{3.9}$$

Why does it make sense in regards to the contour integral? Setting $k_y \to -k_y$, means that we have to draw a contour in the lower half plane for the contour to close the function. But then it is the other pole that is enclosed and the signs cancel out. There is therefore no difference in the transition probability to the first order of moving past a sink or a source. The Stückelberg equation (Eq. 3.8) can therefore be written as,

$$P_+(T) = 2P_{LZ} - 2P_{LZ}^2 + 2P_{LZ}^2\left(P_{LZ}^{-1} - 1\right)\cos(2(\Phi_{dyn}^{(+,-)} + \phi_{st} + \frac{\pi}{2})), \tag{3.10}$$

where $\phi_{st,\alpha}^+ = \phi_{st,\beta}^- + \pi$ (See Appendix 8.D). We can appreciate that it is only the dynamical phase acquired between the nodes, which is relevant, and not the phase acquired after passing the second node. The only

transition allowed is the non adiabatic one, and the only interference is with particles that travel between the bands. Consequently of Eq 3.10 the Landau-Zener-Stückelberg (LZS) probability has two orders of magnitude,

$$P_+(T) = \mathcal{O}(P_{LZ}) + \mathcal{O}(P_{LZ}^2) = 2P_{LZ}(1 + \cos(2(\Phi_{dyn,1} + \phi_{st} + \frac{\pi}{2}))) - 2P_{LZ}^2(1 + \cos(2(\Phi_{dyn,1} + \phi_{st} + \frac{\pi}{2})))$$

$$= 4P_{LZ}(1 - P_{LZ})\cos^2((\Phi_{dyn}^{(+,-)} + \phi_{st} + \frac{\pi}{2})). \tag{3.11}$$

We have also talked, in Sec. 2.2, about the discrepancy between the prefactor in the LZ transition probability that we have calculated, and that calculated exactly with the full higher order solution. The prefactor is explained by [13, 22]: Adiabatic perturbation theory, even for the standard LZ problem will not return the correct prefactor. Instead of looking at the entire adiabatic sum of terms in the perturbation, we solve the problem for the deep adiabatic limit; which is the first order perturbation theory. Consequently, for our approximation to be suitable, we require the gap between the two Bloch bands, $\Delta(\mathbf{k})$, to be much bigger than that of the force in such a way that, $F \ll \Delta(\mathbf{k}) = 2|\mathbf{S}(\mathbf{k})| = 2E_+$. Only evolutions far from the monopole is characterized with this adiabatic perturbation theory. Due to the first order pertubation theory, only small transition amplitudes are appropriate as $A_-(\infty) \simeq 1$. However, in fact the previous inequality is not entirely correct e.g. $F, \Delta$ do not have the same dimensions. I have mentionened it before, in Sec. 2.1.3. The coupling of the adiabatic eigenstates is required to be small:

$$\text{Abs}\left[\langle \psi_+ | \partial_t \psi_- \rangle\right] \ll 1. \tag{3.12}$$

For the three cases this equation correspond to,

$$\text{Abs}\left[\langle \psi_+ | \partial_t \psi_- \rangle\right] = \begin{cases} \dfrac{\partial_t \theta_S}{2} = \dfrac{Fk_{0,\Gamma}^2}{2(F^2 t^2 + k_{0,\Gamma}^4)} = \dfrac{2Fk_{0,\Gamma}^2}{\Delta(\mathbf{k})^2} & \text{move } k_z, \text{ displace } k_y/k_x \\[3mm] \dfrac{\partial_t \theta_S}{2} = \dfrac{F^2 k_{0,z} t}{k_{0,z}^2 + F^4 t^4} = \dfrac{4F^2 k_{0,z} t}{\Delta(\mathbf{k})^2} & \text{move } k_x, \text{ displace } k_z \\[3mm] \dfrac{\partial_t \phi_S}{2} = \dfrac{Fk_{0,y}}{k_{0,y}^2 + F^2 t^2} = \dfrac{2Fk_{0,y}}{\Delta(\mathbf{k})} & \text{move } k_x, \text{ displace } k_y \end{cases} \tag{3.13}$$

The gap also is a function of $F \cdot t$, but we might be better off by exchanging $t \to T'$. That is $T'$ is some period over which the adiabatic theorem breaks down. For the sake of computation we can set $T' = \frac{T_{BZ}}{4} = \frac{\pi}{2F}$, choosing a lattice spacing of 1. If we look at the plots in Fig. 3 we can see that the envelopes changes their realtive positioning in the case of moving in $k_x$ with a displacement in $k_y$. This seems to be an intrinsic property of the double-Weyl nodes, and could very well be used in future experiments. Furthermore, in Appendix 8.F we will look at non-zero temperature non-interacting distrubutions a how they would have evolved after a transport through the $1^{st}$ BZ.

## 3.1 Particle travel back and forth past a Weyl node

The previous section showed the transistion probabilities as the particles travel one full trip through BZ. To check the calculation it is perhaps suited to also show the probability when traveling past one monopole, waiting, and then turning back to the origin, going past the monopole again[25](See Fig. 2). The hermitian conjugate is equivalent to a time reversal.

$$P_+(T) = \left| M_{dyn}^\dagger M_{LZ}^\dagger M_{wait} M_{LZ} M_{dyn} | \psi(t = -\infty) \rangle \right|^2. \tag{3.14}$$

The $M_{wait}$ is the phase acquired when a particle is static in one of the bands for a time $t_{wait}$.

$$M_{wait} = \begin{pmatrix} e^{-iE_- t_{wait}} & 0 \\ 0 & e^{-iE_+ t_{wait}} \end{pmatrix}. \tag{3.15}$$

13

**(a)** Stückelberg probability when moving in $k_x$ with a displacement $k_y = (2, 3, 5)$, plotted against $\frac{1}{F}$.

**(b)** Stückelberg probability when moving in $k_x$ with a displacement $k_z = (1, 2, 3)$, plotted against $\frac{1}{F}$.

**(c)** Stückelberg probability when moving in $k_z$ with a displacement $k_0 = (1, 1.5, 2)$, plotted against $\frac{1}{F}$.
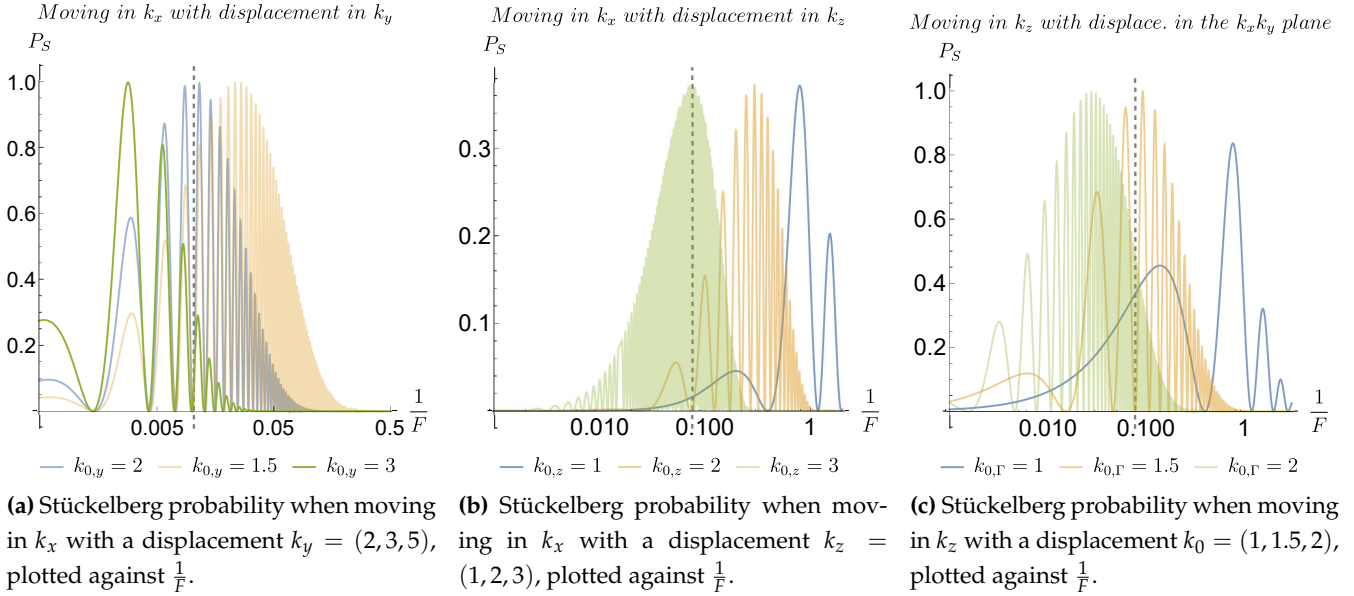
**Figure 3:** Transition probabilities for the three cases of Table 2 plotted against $\frac{1}{F}$. The gray dotted line marks where the adiabatic theorem breaks down from Eq. 3.12. We know that the prefactors of $P_{LZ}$ in Table 2 are wrong, but the specific correction cannot be calculated. In these plots we have therefore set the prefactor to 1, in the same manner as [13]

Due to the fact that it is the same touching point the LZS probability is given by

$$P_+(T) = -4P_{LZ}(P_{LZ} - 1)\sin^2\left(\Delta\phi + \phi_{st}\right), \tag{3.16}$$

where $\Delta\phi = (\Phi_{dyn} + E_+ t_{wait})$ is the phase differences acquired, due to all dynamical factors, that is waiting $t_{wait}$ and accelerating, $\Phi_{dyn}$. The phase is simplified in comparison with the work done by Zenesini et al. [25] by the fact that $E_+ = E_-$.

# 4 The topology of the nodes

This section focuses on explaining the physics of the nodes and their correspondence to the topology of the Hamiltonian. The nodes can be described as constituting synthetic quantum mechanical magnetic monopoles in the reciprocal space [28, 29]. When a particle moves around the nodes, it acquires a Berry phase, which is defined as a path integral of the Berry connection $\mathcal{A}$. The Berry connection of the lower level, is

$$\mathcal{A}_-(\mathbf{S}) = i\langle\psi_-|\nabla_\mathbf{S}\psi_-\rangle. \tag{4.1}$$

simply by using the time-dependent Schrödinger equation[29]. To acquire the field that generates this connection and subsequent phase, in three dimensions, a Berry curvature is defined as the curl of the connection.

$$\mathbf{\Omega}_-(\mathbf{S}) = i \cdot \nabla_\mathbf{S} \times \begin{pmatrix} \langle\psi_-|\partial_S\psi_-\rangle \\ \langle\psi_-|\partial_{\theta_S}\psi_-\rangle \\ \langle\psi_-|\partial_{\phi_S}\psi_-\rangle \end{pmatrix} = \begin{pmatrix} \partial_{\theta_S}A_{\phi_S} - \partial_{\phi_S}A_{\theta_S} \\ \partial_{\phi_S}A_S - \partial_S A_{\phi_S} \\ \partial_S A_{\theta_S} - \partial_{\theta_S}A_S \end{pmatrix}. \tag{4.2}$$

This vector field is generally a tensor; but for non-degenerate systems and due to the 3 dimensionality of our parameter space it reduces to a vector. Unlike the connection this field is gauge invariant, and an actual physical size. It can be checked that the path integral of the connection equals a surface integral around the

node, cf. Stokes Theorem. The states of a two-level Bloch band Hamiltonian do not depend on the size of S, meaning $A_S = 0$ and $\partial_S A_i = 0$,

$$\mathbf{\Omega}_-(\mathbf{S}) = \begin{pmatrix} \partial_{\theta_S} A_{\phi_S} - \partial_{\phi_S} A_{\theta_S} \\ 0 \\ 0. \end{pmatrix}. \tag{4.3}$$

In this parameter space the curvature will act as a monopole.

## 4.1 The Berry monopole in momentum space

The components of S is also dependent on $k_x, k_y, k_z$ or $k, \theta_k, \phi_k$. The Berry connection can then be defined for momentum space. We will derive it for Cartesian and calculate it for spherical coordinates,

$$\mathcal{A}_-(\mathbf{k}) = i\langle \psi_- | \nabla_\mathbf{k} \psi_- \rangle. \tag{4.4}$$

The Berry curvature for the Cartesian case will help us express the anomalous flow in Sec. 4.2, while the flux is easily calculated with the spherical coordinates. Starting with the Cartesian case,

$$\mathcal{A}_-(\mathbf{k}) = i \begin{pmatrix} \langle \psi_- | \partial_{k_x} \psi_- \rangle \\ \langle \psi_- | \partial_{k_y} \psi_- \rangle \\ \langle \psi_- | \partial_{k_z} \psi_- \rangle \end{pmatrix}. \tag{4.5}$$

The differential are substituted to the variable used in the states,

$$\partial_{k_i} = \frac{dS_x}{dk_i}\left(\frac{dS}{dS_x}\partial_S + \frac{d\theta_S}{dS_x}\partial_{\theta_S} + \frac{d\phi_S}{dS_x}\partial_{\phi_S}\right) + \frac{dS_y}{dk_i}\left(\frac{dS}{dS_y}\partial_S + \frac{d\theta_S}{dS_y}\partial_{\theta_S} + \frac{d\phi_S}{dS_y}\partial_{\phi_S}\right) + \frac{dS_z}{dk_i}\left(\frac{dS}{dS_z}\partial_S + \frac{d\theta_S}{dS_z}\partial_{\theta_S} + \frac{d\phi_S}{dS_z}\partial_{\phi_S}\right). \tag{4.6}$$

Naturally the states do not depend on the size of S. It can also be checked that,

$$\langle \psi_- | \partial_{\theta_S} \psi_- \rangle = 0, \qquad\qquad \langle \psi_- | \partial_{\phi_S} \psi_- \rangle = \frac{i}{2}\cos(\theta_S), \tag{4.7}$$

meaning that

$$\mathcal{A}_{cart}(\mathbf{k}) = -\frac{1}{2}\cos(\theta_S) \begin{pmatrix} \frac{dS_x}{dk_x}\frac{d\phi_S}{dS_x} + \frac{dS_y}{dk_x}\frac{d\phi_S}{dS_y} \\ \frac{dS_x}{dk_y}\frac{d\phi_S}{dS_x} + \frac{dS_y}{dk_y}\frac{d\phi_S}{dS_y} \\ \frac{dS_z}{dk_z}\frac{d\phi_S}{dS_z} \end{pmatrix} = \frac{-\cos(\theta_S)}{S_x\left(\frac{S_y^2}{S_x^2}+1\right)} \begin{pmatrix} k_y - k_x\frac{S_y}{S_x} \\ k_x - k_y\frac{S_y}{S_x} \\ 0 \end{pmatrix}. \tag{4.8}$$

The Berry curvature equation (Eq. 4.2) yields

$$\mathbf{\Omega}(\mathbf{k}) = \nabla \times \mathcal{A} = \begin{pmatrix} -\partial_{k_z}A_y(\mathbf{k}) \\ \partial_{k_z}A_x(\mathbf{k}) \\ \partial_{k_x}A_y(\mathbf{k}) - \partial_{k_y}A_x(\mathbf{k}) \end{pmatrix}. \tag{4.9}$$

The first two coordinates are trivial to calculate, as the only $k_z$ dependent parameter for $\mathcal{A}_{cart}$ is $\cos(\theta_S)$:

$$\partial_{k_z}\cos(\theta_S) = \frac{dS_z}{dk_z}\partial_{S_z}\cos(\theta_S) = \partial_{S_z}\frac{S_z}{\sqrt{S_z^2 + S_y^2 + S_x^2}} = \frac{1}{E_+}(1 - \cos^2(\theta_S)). \tag{4.10}$$

The $\Omega_{k_x/k_y}$ is then,

$$\Omega_{k_x} = \frac{k_x - k_y\frac{S_y}{S_x}}{S_x\left(\frac{S_y^2}{S_x^2}+1\right)E_+}(1 - \cos^2(\theta_S)), \qquad\qquad \Omega_{k_y} = -\frac{k_y - k_x\frac{S_y}{S_x}}{S_x\left(\frac{S_y^2}{S_x^2}+1\right)E_+}(1 - \cos^2(\theta_S)). \tag{4.11}$$

The last coordinate is a bit more brute force method. It reduces to

$$\Omega_{k_z}(\mathbf{k}) = \frac{k_z}{(k_x^2 + k_y^2)^3 |\mathbf{k}|^3} \left( k_x^6 - 13k_x^4 k_y^2 - 9k_x^2 k_y^4 - 12k_x^2 k_y^2 k_z^2 + 5k_y^6 + 4k_y^2 k_z^2 \right) \tag{4.12}$$

Using exactly the same method, but now for spherical momentum coordinates the Berry connection and curvature is found as

$$\mathcal{A} = \frac{\cos(\theta_S)}{k \sin(\theta_k)} \boldsymbol{\phi}_{\mathbf{k}} \tag{4.13}$$

$$\boldsymbol{\Omega}(\mathbf{k}) = \frac{1}{k^2 \sin(\theta_k)} \partial_{\theta_k} \cos(\theta_S) \hat{\mathbf{k}} - \frac{1}{k \cdot \sin(\theta_k)} \partial_k \cos(\theta_S) \hat{\boldsymbol{\theta}}_k \tag{4.14}$$

Equipped with these equations we calculate the Berry flux of these Berry curvatures in Appendix 4. This is either done by integrating over the surface of a sphere in the case of the spherical Berry curvature, or two infinitely large planes on either side of the node, in the Cartesian case. The result is that the two equations constitute double-Weyl nodes with a Chern number of 2.

## 4.2 Anomalous flow

We will prove that there is no movement in real space as the atoms make one round-trip of the BZ. The two cases investigated in this paper is

$$\mathbf{F} = \begin{cases} \mathbf{F}_x = F \cdot \hat{\mathbf{x}} = k_x \cdot \hat{\mathbf{x}} \\ \mathbf{F}_z = F \cdot \hat{\mathbf{z}} = k_z \cdot \hat{\mathbf{z}} \end{cases} \tag{4.15}$$

As such two cases of anomalous velocities could be calculated. The anomalous velocity is due to the breaking of translational symmetry caused by applying a force of F [29]. To satisfy Bloch's theorem the actual momentum we have discussed is the gauge invariant momentum. Instead, while the the physical momentum is a constant of motion, the gauge invariant momentum changes as we move through the BZ. This we will now see. Firstly the case of moving in $k_z$

$$\partial_t r = \nabla_{\mathbf{k}} E(\mathbf{k}) + \mathbf{F}_z \times \boldsymbol{\Omega} = \nabla_{\mathbf{k}} E(\mathbf{k}) - F \begin{pmatrix} \partial_z A_x(\mathbf{k}) \\ \partial_{k_z} A_y(\mathbf{k}) \\ 0 \end{pmatrix} \tag{4.16}$$

and in the case of moving in $k_x$

$$\partial_t r = \nabla_{\mathbf{k}} E(\mathbf{k}) + \mathbf{F}_x \times \boldsymbol{\Omega} = \nabla_{\mathbf{k}} E(\mathbf{k}) + F \begin{pmatrix} 0 \\ \partial_{k_y} A_x(\mathbf{k}) - \partial_{k_x} A_y(\mathbf{k}) \\ \partial_{k_z} A_x(\mathbf{k}) \end{pmatrix} \tag{4.17}$$

The velocity of each state $\mathbf{k}$ corresponds to the change of the Berry curvature. As the trip is through the entire BZ, the energy gradient will average to zero. However the anomalous term will contribute with a velocity perpendicular to the direction of the force. The distance covered is found by an integration of the velocity as a function the momentum $\int_{k_0}^{k_0 + 2\pi} dk_i \partial_t r$

**Moving in $k_x$:** The integration yields a movement in

$$dr_z = \int_{k_0}^{k_0+2\pi} dk_x \partial_{k_z} A_x(\mathbf{k}), \qquad dr_y = \int_{k_0}^{k_0+2\pi} dk_x \left[ \partial_{k_y} A_x(\mathbf{k}) - \partial_{k_x} A_y(\mathbf{k}) \right] \tag{4.18}$$

$$= \int_{k_0}^{k_0+2\pi} dk_x \partial_{k_y} A_x(\mathbf{k}) - \left[ A_y(\mathbf{k}) \right]_{k_0}^{k_0+2\pi} \tag{4.19}$$

**Moving in $k_z$:** The integration yields a movement in

$$dr_x = \int_{k_0}^{k_0+2\pi} dk_z \partial_{k_z} A_x(\mathbf{k}) = \left[A_x(\mathbf{k})\right]_{k_0}^{k_0+2\pi}, \qquad dr_y = \int_{k_0}^{k_0+2\pi} dk_z \partial_{k_z} A_y(\mathbf{k}) = \left[A_y(\mathbf{k})\right]_{k_0}^{k_0+2\pi} \tag{4.20}$$

The Berry connection is periodic when we move the atom through the entire BZ. The only anomalous velocity will then appear for the movement in $\hat{\mathbf{x}}$

$$\mathbf{dr} = \begin{pmatrix} 0 \\ \int_{k_0}^{k_0+2\pi} dk_x \partial_{k_y} A_x(\mathbf{k}) \\ \int_{k_0}^{k_0+2\pi} dk_x \partial_{k_z} A_x(\mathbf{k}) \end{pmatrix} \tag{4.21}$$

Until now, the Hamiltonian, from where our eigenstates are derived, has not been dealing with the periodicity of the BZ. The more general lattice Hamiltonian, from where we can derive the effective Hamiltonian (Eq. 2.1) is:

$$\mathcal{H} = -(\cos(k_x)^2 - \cos(k_y)^2)\sigma_x + 2\sin(k_x)\sin(k_y)\sigma_y + \sin(k_z)\sigma_z \tag{4.22}$$

Integration of the derivative of the x-component of Eq. 4.8, using the lattice Hamiltoninan yields a zero in both direction of Eq. 4.21

# 5 Higher order perturbation theory

With the first order TDPT results of the LZ transition from Sec. 2, we will conclude this thesis' results by analyzing a more general way to derive higher order terms in the perturbation theory. The method is based on the work by Rojo [20]. The explicit evaluation of the integral is left for future investigation.

## 5.1 The standard Landau-Zener problem

The method is presented by the paper of Rojo [20]. In our system, the case of moving in the $k_z$ direction the analogy to that of the standard LZ problem. A unitary tranformation, $U$ (See Appendix 8.B), of the Hamiltonian in Eq. 2.7 yields,

$$\tilde{\mathcal{H}} = U^\dagger H U - U^\dagger \partial_t U, = \begin{pmatrix} 0 & \Gamma e^{-iFt^2/2} \\ \Gamma^* e^{iFt^2/2} & 0 \end{pmatrix}, \qquad U = e^{i\sigma_z \int^t dt' Ft}. \tag{5.1}$$

The fact that this linear case Hamiltonian acquires only off-diagonal terms means that only integrals with an odd number of Hamiltonians will count in the evaluation of the upper band states in our perturbation theory's Dyson series.

$$\begin{pmatrix} A_+(\infty) \\ A_-(\infty) \end{pmatrix} = \mathcal{T}_n \left[e^{i\int dt \tilde{H}(t)}\right] \begin{pmatrix} A_+(-\infty) \\ A_-(-\infty) \end{pmatrix} \tag{5.2}$$

Note the alternating sign of the exponential in the integral, for each of the $dt_n$-integrals in the time-ordered integral, $T_n$. We also employ the use of the Heavyside function in its integral form,

$$\Theta(t) = \frac{1}{2i\pi} \int_{-\infty}^{\infty} d\omega \frac{e^{i\omega t}}{\omega + i\epsilon}, \tag{5.3}$$

as an integral of frequency $\omega$. This means that instead of having differing integral limits, dependent on each other, all integrals will run over the same interval, and the Heavyside function will act as the boundary of integrals. The solution can then be found with the Dyson series [17]

$$A_+(\infty) = \sum_{n=0}^{\infty} (-1)^n \left[\frac{|\Gamma|}{F}\right]^{2n} \frac{\Gamma}{F} T_{2n+1} \quad , \quad n = [0, 1, 2...], \tag{5.4}$$

where the odd-sized timeordered integral, $T_{2n+1}$, with alternating functions is,

$$T_{2n+1} = \frac{1}{(2i\pi)^{2n}} \int_{-\infty}^{\infty} \left( \prod_{i=1}^{2n+1} t_i \right) \int_{-\infty}^{\infty} \left( \prod_{j=1}^{2n} \omega_j \right) \frac{e^{it_1^2} e^{i\omega_1(t_1-t_2)}}{\omega_1 + i\epsilon} \frac{e^{-it_2^2} e^{i\omega_2(t_2-t_3)}}{\omega_2 + i\epsilon} \cdots \frac{e^{-it_{2n+1}^2} e^{i\omega_{2n}(t_{2n}-t_{2n+1})}}{\omega_{2n} + i\epsilon} \tag{5.5}$$

Because we are now dealing with the standard LZ problem this integral is somewhat simple to solve. Solving the square to get gaussian time-integrals[1] yields,

$$\int dt e^{\pm it^2} = \sqrt{\frac{\pi}{\pm i}}. \tag{5.6}$$

The timeordered integral is now a function of new Heavyside functions, by relabeling the indices of $\omega_i$. This yields identical integrals, $I_1$. A product of n identical integrals, $I_n$, can be written as

$$I_n = \frac{1}{n!} \left( \int dt I_1(t) \right)^n. \tag{5.7}$$

We will skip to the final result which is the well-known LZ probability of Eq. 2.13. To see the last equations where the sum is gathered and converged we refer to [20].

## 5.2 Quadratic dispersion in the Landau-Zener problem

Insteadof describing the linear case we will spend more time on describing the problem for the Hamiltonian of Eq. 2.14, which is more complex. A pseudo-rotation using a unitary transformation, $U_\circ$, yields:

$$U_\circ = (\sqrt{2})^{-1} \begin{pmatrix} 1 & 1 \\ 1 & -1 \end{pmatrix}, \quad \Rightarrow \quad H = \begin{pmatrix} F^2 t^2 & k_z \\ k_z & -F^2 t^2 \end{pmatrix} \tag{5.8}$$

Another unitary transformation yields the diagonal Hamiltonian,

$$U = e^{i\sigma_z \int^t dt' F^2 t^2}, \quad \Rightarrow \quad \tilde{\mathcal{H}} = \begin{pmatrix} 0 & k_{0,z} e^{-2iF^2 t^3/3} \\ k_{0,z} e^{2iF^2 t^3/3} & 0 \end{pmatrix}. \tag{5.9}$$

The exponential in the time-ordered integral can be simplified like the previous section by a change of integration variable, $t' = \sqrt[3]{\frac{2}{3}} F^{2/3} t$. Our time-ordered exponential integral is,

$$\begin{pmatrix} A_+(\infty) \\ A_-(\infty) \end{pmatrix} = \mathcal{T} \left[ e^{i \int_{-\infty}^{\infty} H(t) dt} \right] \begin{pmatrix} A_+(-\infty) \\ A_-(-\infty) \end{pmatrix} \tag{5.10}$$

Since the Hamiltonian is off-diagonal, we only need the odd terms in the time-ordered integral, $T_{2n+1}$,

$$T_{2n+1} = \left( \sqrt[3]{\frac{3}{2}} F^{3/2} \right)^{2n+1} \int_{-\infty}^{\infty} \int_{-\infty}^{t_1} \cdots \int_{-\infty}^{t_{2n+1}} \left( \prod_{i=0}^{2n+1} dt_i \right) e^{-it_1^3 + it_2^3 - it_3^3 + \ldots - it_{2n+1}^3}. \tag{5.11}$$

The Dyson series that yields the amplitude of the upper band now reads,

$$A_+(\infty) = i \sum_{n=0}^{\infty} (-1)^n \left( \sqrt[3]{\frac{3}{2}} F^{3/2} k_{0,z} \right)^{2n+1} T_{2n+1}. \tag{5.12}$$

This timeordered integral is not Gaussian. To solve the integrals, we shift the origin of time from $t = -\infty \to t = 0$ without the loss of generality, and the Heavyside function in its intgral form is introduced again to control the bounds of the integral

$$T_{2n+1} = \frac{1}{(2\pi i)^{2n}} \int_0^{\infty} \left( \prod_i^{2n+1} dt_i \right) \int_{-\infty}^{\infty} \left( \prod_j^{2n} d\omega_j \right) \frac{e^{it_1^3} e^{i\omega_1(t_1-t_2)}}{\omega_1 + i\epsilon} \frac{e^{-it_2^3} e^{i\omega_2(t_2-t_3)}}{\omega_2 + i\epsilon} \cdots \frac{e^{-it_{2n+1}^3} e^{i\omega_{2n}(t_{2n}-t_{2n+1})}}{\omega_{2n} + i\epsilon} \tag{5.13}$$

---

[1]The center of the curve is displaced, however the integral runs from $-\infty$ to $\infty$

The time-ordered integral is now a product of integrals. We will now draw the $2\pi i$-term into the sum of Eq. 5.12. The starting general $I_1$, ending integral $I_{2n+1}$, and general integrals $I_{j,\pm}$ to solve are,

$$I_1(\omega_1) = \int_0^\infty dt_1 e^{-t_1^3 + i\omega_1 t_1}, \qquad\qquad I_{2n+1}(i\omega_{2n}) = \int_0^\infty dt_{2n+1} e^{-t_{2n+1}^3 - i\omega_{2n} t_{2n+1}},$$

$$I_{j,\pm}((\omega_j - \omega_{j-1})) = \int_0^\infty dt_j e^{\pm i t_j^3 + i(\omega_j - \omega_{j-1})t_j} \tag{5.14}$$

The solution is obtained with the mathematica integration tool:

$$I_{j,+}(\omega) = \int_0^\infty dt_j e^{i t_j^3 + i(\omega)t_j} = \frac{2\pi}{3\sqrt[3]{3}} e^{\frac{\pi i}{6}} \mathrm{Bi}\left[\frac{\omega}{\sqrt[3]{3}} e^{\frac{2\pi i}{3}}\right] - i\frac{\omega^2}{6} {}_1 F_2\left[1; \frac{4}{3}, \frac{5}{3}; \left(\frac{\omega}{3}\right)^3\right] \tag{5.15}$$

While the minus integral can be written as

$$I_-(\omega) = \frac{2\pi\sqrt{\omega}e^{-i\pi/6} J_{-1/3}\left[\frac{2\omega^{3/2}}{3\sqrt{3}}\right]}{9} + \frac{2\pi\sqrt{\omega}e^{i\pi/6} J_{1/3}\left[\frac{2\omega^{3/2}}{2\sqrt{3}}\right]}{9}$$
$$+ \frac{i\omega^2}{6} {}_1 F_4\left[1; \frac{2}{3}, \frac{5}{6}, \frac{7}{6}, \frac{4}{3}; \left(\frac{\omega}{3(2)^{3/2}}\right)^6\right] - \frac{i\omega^5}{360} {}_1 F_4\left[1; \frac{7}{6}, \frac{4}{3}, \frac{5}{3}, \frac{11}{6}; \left(\frac{\omega}{3(2)^{3/2}}\right)^6\right] \tag{5.16}$$

The result is a mixture of second kind Airy ($Bi(z)$), Bessel ($J_i(z)$), and generalized hypergeometric functions ($_q F_p\left[\mathbf{a}_q; \mathbf{b}_p; z\right]$). The now frequency-ordered integral yields, without the fraction $\frac{1}{\omega_i - i\epsilon}$,

$$T_{2n+1} = \int_{-\infty}^\infty \left(\prod_j d\omega_j\right) I_1(\omega_1) \cdot I_{2,-}(\omega_2 - \omega_1) \cdot \prod_{i,k=2}^{n-1}\left[I_{2k-1,+}(\omega_{2i-1} - \omega_{2i-2}) \cdot I_{2k,-}(\omega_{2i} - \omega_{2i-1})\right],$$

$$\cdot I_{2n,+}(\omega_{2n} - \omega_{2n-1}) \cdot I_{2n+1}(-\omega_{2n}). \tag{5.17}$$

To solve this integral, we use a convolution of the functions. The integrals as a function of $\omega$ can be viewed in Appendix 8.G. The complexity consists in the fact that the integration is over functions that have connected variables. A way to proceed is via the Fourier transform ($\mathcal{F}[f(x)] = \tilde{f}(\phi)$) convolution theorem. We reintroduce the fraction $\frac{1}{\omega_i - i\epsilon}$,

$$I_{con,\omega_2}(\omega_2) = \int_{-\infty}^\infty \frac{I_1(\omega_1)}{\omega_1 - i\epsilon} I_{2,-}(\omega_2 - \omega_1) d\omega_1,$$

$$I_{con,\omega_3}(\omega_3) = \int_{-\infty}^\infty \frac{I_{con,\omega_2}(\omega_2)}{\omega_2 - i\epsilon} I_{3,+}(\omega_3 - \omega_2) d\omega_2,$$

$$\vdots$$

$$T_{2n+1} = \int_{-\infty}^\infty \frac{I_{con,\omega_{2n}}(\omega_{2n})}{\omega_{2n} - i\epsilon} I_{2n+1}(-\omega_{2n}) d\omega_{2n} \tag{5.18}$$

The problem is that we do not know the answer to this recursive formula. However we might choose to use the theorem,

$$h(z) = \int_{-\infty}^\infty f(z)g(z + x)dz \to \mathcal{F}[h](\phi) = \sqrt{2\pi}\mathcal{F}[f](\phi)\mathcal{F}[g](\phi) \tag{5.19}$$

This we will use

$$\mathcal{F}\left[I_{con,\omega_2}\right](\phi) = \sqrt{2\pi}\mathcal{F}\left[\frac{I_1(\omega_1)}{\omega_1 - i\epsilon}\right]\mathcal{F}\left[I_{2,-}(\omega_2 - \omega_1)\right]$$

$$\mathcal{F}\left[I_{con,\omega_3}\right](\phi) = \sqrt{2\pi}\mathcal{F}\left[\frac{I_{con,\omega_2}(\omega_2)}{\omega_2 - i\epsilon}\right]\mathcal{F}\left[I_{3,+}(\omega_3 - \omega_2)\right]\dots \tag{5.20}$$

Applying the convolution theorem again

$$\mathcal{F}\Big[T_{2n+1}\Big](\phi)\prod_{j=1}^{2n}\mathcal{F}\Big[\omega_j-i\epsilon\Big]=(2\pi)^n\mathcal{F}\Big[I_1(\omega_1)\Big]\mathcal{F}\Big[I_{2n+1}(\omega_{2n})\Big]\prod_{i=1}^{n}\mathcal{F}\Big[I_{2i,-}(\omega_{2i}-\omega_{2i-1})\Big]\cdot\mathcal{F}\Big[I_{2i,+}(\omega_{2i+1}-\omega_{2i})\Big] \tag{5.21}$$

While we now have derived the formula for the Fourier transform of the time-ordered integral, we have not gained any insight. The functions are not that easily transformed, and to obtain the time-ordered integral we have to deconvolute $\mathcal{F}\big[T_{2n}\big]$ again. If we could succeed in this, the only step missing would be to find the convergence of the Dyson series, which is the amplitude, $A_+(\infty)$. We cannot obtain a unitary transform of the kind in Eq. 5.9 for movement in $k_x$ and a displacement in $k_y$. Due to the quadratic element, both Pauli matrices has the time dependency. This mixing between the two, results in the fact that a rotation of the Bloch sphere (Appendix 8.C, Fig 4) will leave some time dependency in the factor infront of the exponential.

# 6    Conclusion

This thesis has shown that the method of Landau-Zener-Stückelberg, is applicable for a quantum simulation of a double-Weyl semimetal. The quadratic dispersions in the Hamiltonian is still solvable by a first order approximation as suggested in the work of Montabaux et al. [13, 21] (See Table 2). We have presented the Stückelberg probability plots in Fig. 3. Higher order corrections as shown in [20] by Rojo can be achieved for two of the cases of a displacement from the Weyl node; namely the case of moving in $k_x, k_y$ with a displacement in $k_z$ and moving in $k_z$ with a displacement in $k_x, k_y$-plane. However, we did not aquire the full equation for transitions from the recursive formula in the case of moving in $k_x, k_y$ with a displacement in $k_z$. We have also discussed the consequnce of a system with two double-Weyl nodes, effectively breaking the $O(2)$ symmetry and going to a $C_4$ symmetry, by adding a small anisotropical term by the one double-Weyl node. Approximately, we add a term in the energy, linear in the anisotropy, that has singular points in the complex plane.

For further research it would also be satisfactory to discuss the the limit of extreme diabacity. For faster moving systems in the vicinity of crossing the diabatic basis is more suitable [13]. However, another way to express the diabatic case is to see the Bloch bands as degenerate [30, 29,(*Chap. IX*)]. This is a more complex situation, where our semiclassical approach breaks down. In the degenerate case, we can no longer draw parallels between the Berry connection and curvature and the magnetic vector potential and field strength. Instead the two are matrices of vectors, where they correspond to the gauge potential and the gauge field in SU(2) gauge theory [29]. The Berry phases of the adiabatic case convert to a non-Abelian phase. To this we refer to the Berry conection:

$$\mathcal{A}_{ij}=\langle\psi_i|\partial_S\psi_j\rangle \tag{6.1}$$

The topology of the system can be researched further. From this alot of transport theory of atoms in the system can be explored.

# Acknowledgement

# 7 References

[1] C. Gross and I. Bloch. Quantum simulations with ultracold atoms in optical lattices. Science, 357:995–1001, September 2017. doi: 10.1126/science.aal3837.

[2] H. Gao, J. W. F. Venderbos, Y. Kim, and A. M. Rappe. Topological Semimetals from first-principles. Annual Review of Condensed Matter Physics, October 2018.

[3] A. A. Burkov. Weyl Metals. Annual Review of Condensed Matter Physics, 9:359–378, March 2018. doi: 10.1146/annurev-conmatphys-033117-054129.

[4] L. Lepori, I. C. Fulga, A. Trombettoni, and M. Burrello. Double Weyl points and Fermi arcs of topological semimetals in non-Abelian gauge potentials. Physical Review Letters, 94(5):053633, November 2016. doi: 10.1103/PhysRevA.94.053633.

[5] H. Miyake, G. A. Siviloglou, C. J. Kennedy, W. C. Burton, and W. Ketterle. Realizing the Harper Hamiltonian with Laser-Assisted Tunneling in Optical Lattices. Physical Review Letters, 111(18):185302, November 2013. doi: 10.1103/PhysRevLett.111.185302.

[6] M. Aidelsburger, M. Atala, M. Lohse, J. T. Barreiro, B. Paredes, and I. Bloch. Realization of the Hofstadter Hamiltonian with Ultracold Atoms in Optical Lattices. Physical Review Letters, 111(18):185301, November 2013. doi: 10.1103/PhysRevLett.111.185301.

[7] Yasumasa Hasegawa. Generalized flux states on 3-dimensional lattice. Journal of the Physical Society of Japan, 59(12):4384–4393, 1990. doi: 10.1143/JPSJ.59.4384. URL https://doi.org/10.1143/JPSJ.59.4384.

[8] L. Henriet. Geometrical properties of the ground state manifold in the spin boson model. Physical Review Letters, 97(19):195138, May 2018. doi: 10.1103/PhysRevB.97.195138.

[9] M Burrello, I C Fulga, L Lepori, and A Trombettoni. Exact diagonalization of cubic lattice models in commensurate abelian magnetic fluxes and translational invariant non-abelian potentials. Journal of Physics A: Mathematical and Theoretical, 50(45):455301, oct 2017. doi: 10.1088/1751-8121/aa8d26. URL https://doi.org/10.1088.

[10] N. Goldman, F. Gerbier, and M. Lewenstein. Realizing non-Abelian gauge potentials in optical square lattices: an application to atomic Chern insulators. Journal of Physics B Atomic Molecular Physics, 46(13):134010, July 2013. doi: 10.1088/0953-4075/46/13/134010.

[11] T. Dubček, C. J. Kennedy, L. Lu, W. Ketterle, M. Soljačić, and H. Buljan. Weyl Points in Three-Dimensional Optical Lattices: Synthetic Magnetic Monopoles in Momentum Space. Physical Review Letters, 114(22):225301, June 2015. doi: 10.1103/PhysRevLett.114.225301.

[12] X.-Y. Mai, D.-W. Zhang, Z. Li, and S.-L. Zhu. Exploring topological double-Weyl semimetals with cold atoms in optical lattices. Physical Review Letters, 95(6):063616, June 2017. doi: 10.1103/PhysRevA.95.063616.

[13] J.-N. Fuchs, L.-K. Lim, and G. Montambaux. Interband tunneling near the merging transition of Dirac cones. Physical Review Letters, 86(6):063613, December 2012. doi: 10.1103/PhysRevA.86.063613.

[14] L. Tarruell, D. Greif, T. Uehlinger, G. Jotzu, and T. Esslinger. Creating, moving and merging Dirac points with a Fermi gas in a tunable honeycomb lattice. Nature, 483:302–305, March 2012. doi: 10.1038/nature10871.

[15] C. Zener. Non-Adiabatic Crossing of Energy Levels. Proceedings of the Royal Society of London Series A, 137:696–702, September 1932. doi: 10.1098/rspa.1932.0165.

[16] Curt Wittig. The landau - zener formula. The Journal of Physical Chemistry B, 109(17):8428–8430, 2005. doi: 10.1021/jp040627u. URL https://doi.org/10.1021/jp040627u. PMID: 16851989.

[17] J. J. Sakurai and J. Napolitano. Modern Quantum Mechanics. September 2017.

[18] A. Zenesini, H. Lignier, G. Tayebirad, J. Radogostowicz, D. Ciampini, R. Mannella, S. Wimberger, O. Morsch, and E. Arimondo. Time-Resolved Measurement of Landau-Zener Tunneling in Periodic Potentials. Physical Review Letters, 103(9):090403, August 2009. doi: 10.1103/PhysRevLett.103.090403.

[19] J. P. Davis and P. Pechukas. Nonadiabatic transitions induced by a time-dependent Hamiltonian in the semi-classical/adiabatic limit: The two-state case. The Journal of Chemical Physics, 64:3129–3137, April 1976. doi: 10.1063/1.432648.

[20] A. G. Rojo. Matrix exponential solution of the Landau-Zener problem. arXiv e-prints, April 2010.

[21] L.-K. Lim, J.-N. Fuchs, and G. Montambaux. Bloch-Zener Oscillations across a Merging Transition of Dirac Points. Physical Review Letters, 108(17):175303, April 2012. doi: 10.1103/PhysRevLett.108.175303.

[22] M. V. Berry and K. E. Mount. Semiclassical approximations in wave mechanics. Reports on Progress in Physics, 35:315–397, January 1972. doi: 10.1088/0034-4885/35/1/306.

[23] Abraham J. Olson, David B. Blasing, Chunlei Qu, Chuan-Hsun Li, Robert J. Niffenegger, Chuanwei Zhang, and Yong P. Chen. Stueckelberg interferometry using periodically driven spin-orbit-coupled bose-einstein condensates. Phys. Rev. A, 95:043623, Apr 2017. doi: 10.1103/PhysRevA.95.043623. URL https://link.aps.org/doi/10.1103/PhysRevA.95.043623.

[24] Plötz, P. and Wimberger, S. Stückelberg-interferometry with ultra-cold atoms. Eur. Phys. J. D, 65(1), 2011. doi: 10.1140/epjd/e2011-10711-6. URL https://doi.org/10.1140/epjd/e2011-10711-6.

[25] A. Zenesini, D. Ciampini, O. Morsch, and E. Arimondo. Observation of Stückelberg oscillations in accelerated optical lattices. Physical Review Letters, 82(6):065601, December 2010. doi: 10.1103/PhysRevA.82.065601.

[26] S. N. Shevchenko, S. Ashhab, and F. Nori. Landau-Zener-Stückelberg interferometry. Journal of Physical Reports, 492:1–30, July 2010. doi: 10.1016/j.physrep.2010.03.002.

[27] J. Lehto and K.-A. Suominen. Superparabolic level-glancing models for two-state quantum systems. Phys. Rev. A, 86(3):033415, September 2012. doi: 10.1103/PhysRevA.86.033415.

[28] T. Dubček, C. J. Kennedy, L. Lu, W. Ketterle, M. Soljačić, and H. Buljan. Weyl Points in Three-Dimensional Optical Lattices: Synthetic Magnetic Monopoles in Momentum Space. Physical Review Letters, 114(22):225301, June 2015. doi: 10.1103/PhysRevLett.114.225301.

[29] D. Xiao, M.-C. Chang, and Q. Niu. Berry phase effects on electronic properties. Reviews of Modern Physics, 82:1959–2007, July 2010. doi: 10.1103/RevModPhys.82.1959.

[30] T. Li, L. Duca, M. Reitter, F. Grusdt, E. Demler, M. Endres, M. Schleier-Smith, I. Bloch, and U. Schneider. Bloch state tomography using Wilson lines. Science, 352:1094–1097, May 2016. doi: 10.1126/science.aad5812.

[31] C. J. Foot. Atomic Physics. Oxford University Press, 2005.

[32] Adri B. Olde Daalhuis, Stephen Chapman, John R. King, John R. Ockendon, and Richard Tew. Stokes phenomenon and matched asymptotic expansions. SIAM Journal of Applied Mathematics, 55:1469–1483, 12 1995. doi: 10.1137/S0036139994261769.

[33] M. O. González. Elliptic Integrals in Terms of Legendre Polynomials. Proceedings of the Glasgow Mathematical Association, 2(2):97–99, 1954. doi: 10.1017/S2040618500033104.

# 8    Appendices

## 8.A    Defining the adiabatic limit and the level lines

This appendix defines the adiabatic limit and describes the branch cuts of the Hamiltonian following the notation and conventions of [19]. We define a generic two level Hamiltonian $H(t)$, which does not cross at any point on the real time axis. For the case of Eq. 2.1 this is achieved by simply displacing the system from the level crossing by some $k_0$. The description of this system adiabatically is the same as the semi-classical limit; that is to say that moving infinitely slow and setting $\hbar = 1$ is the same as the limit $\hbar \rightarrow 0$. Varying

infinitely slowly is achieved with an adiabacity parameter $\delta$ so that in the limit $\delta \to 0$ for $\mathcal{H}_\delta(t) = \mathcal{H}(\delta t)$ fulfills

$$i\partial_t \phi(t, \delta) = \mathcal{H}_\delta(t)\phi(t, \delta) \qquad \Leftrightarrow \qquad i\partial_t \psi(t, \hbar) = \mathcal{H}(t)\psi(t, \hbar) \qquad \text{if } \psi(t, \hbar) = \phi(t/\hbar, \hbar) \tag{8.A.1}$$

This entire thesis is based on the fact that our evolutions can simply be equated by the same method as that of a non-adiabatic transistion at one point and adiabatic evolution everywhere else. Now we want to describe how this is true. The phase - the integral in the exponent - has to account for the branches eminating from the complex crossing points. What we will find is that asymptotically to the first order this is equivalent to integrating to the complex crossing time and moving the exponent out of the $dt$-integral. In these points the energy difference is close to zero, and a Taylor expansion for the two poles reads,

$$2E_+(t) = \delta E(t) = \sqrt{(t - t_c)(t + t_c)} = \alpha(t - t_c)^{1/2}(1 + \beta(t)(t - t_c)) \tag{8.A.2}$$

With some parameter $\alpha$ and function $\beta$. The phase is defined by

$$\Delta(t) = \int^t dt' \delta E(t) \tag{8.A.3}$$

The level lines are defined as the lines where $\Im[\Delta(t)]$ has the same value. The lines that are eminating from a crossing point is called Stoke lines. From the Taylor expansion it can be seen that there are three lines from each point.

$$\Delta(t) = \Delta(t_0) + \frac{2}{3}\alpha(t - t_c)^{3/2} \tag{8.A.4}$$

where we ignore the 5/2 power from the integral, for a small displacement from the singular pole. By this notion we will arrive at [19, Eq 4.23]. Instead of using the eigenstates from a Hamilitonian where $H_{12} = H_{21}$

$$|\psi_-\rangle = \begin{pmatrix} \sin(\theta_S/2) \\ -\cos(\theta_S/2) \end{pmatrix} \quad , \quad |\psi_+\rangle = \begin{pmatrix} \cos(\theta_S/2) \\ \sin(\theta_S/2) \end{pmatrix} \tag{8.A.5}$$

For the movement in $k_x$ and with a displacement in $k_y$, the relation between them is $H_{12} = H_{21}^*$ the eigenstates are that of Eq. 2.2. For movement in $k_x$ and a displacement in $k_y$ it is the exact same scenario.

**4 poles in the Argand plane:** In this case the energy expansion of Eq. 8.A.2 will read.

$$\delta E(t) = \sqrt{(t - t_{c,1})(t + t_{c,1})(t - t_{c,2})(t + t_{c,2})} \tag{8.A.6}$$

With the poles $t_{c,1}, t_{c,2}$However, if we look near the pole, only that pole's value will effectively contribute to the energy

$$\delta E(t) = \sqrt{(t - t_{c,1})(t + t_{c,1})(t - t_{c,2})(t + t_{c,2})} \Rightarrow \delta E(t) = \sqrt{(t - t_{c,1\vee2})(t + t_{c,1\vee2})} \tag{8.A.7}$$

What we find is that even for several poles in the Argand plane we still have an equivalent situation as in [19], and the introduction of complex exponentials to the states, will not play a role. In the work of [19] it is concluded that, for the first order calculation, asymptotically we can ignore the branch cuts.

## 8.B A unitary transformation / The interaction picture

Unitary transformation are of great importance in quantum mechanics[17, Chap. 5.5]. The interaction picture is a result of an unitary tranformation of the Schrödinger picture

$$H_I = U H_S U^\dagger, \quad |\psi\rangle_I = U|\psi\rangle_S \tag{8.B.1}$$

The Schrödinger equation reads

$$\text{Schrödinger Picture: } i\partial_t|\psi\rangle_S = H_S|\psi\rangle_S \Rightarrow$$
$$\text{Interaction Picture: } i\partial_t|\psi\rangle_I = H_I|\psi\rangle_I,$$
$$i\partial_t(U)|\psi\rangle_S + iU\partial_t|\psi\rangle_S = UH_SU^\dagger U|\psi\rangle_S,$$
$$iU^\dagger\partial_t(U)|\psi\rangle_S + i\partial_t|\psi\rangle_S = H_S|\psi\rangle_S, \tag{8.B.2}$$

which motivates that the transformation also can be written as

$$\widetilde{H} = UHU^\dagger + iU^\dagger\partial_t U \tag{8.B.3}$$

## 8.C The Bloch sphere / two-level system

The Bloch sphere is a way to gain a geometric intuition about two level systems[2] [31, Chap. 7.3]. The idea is to visualize the superposition of eigenstates as points on the unit sphere. The north- and southpole then corresponds to the orthonormal eigenstates (See Fig. 4). The reason that the Bloch sphere is such a strong
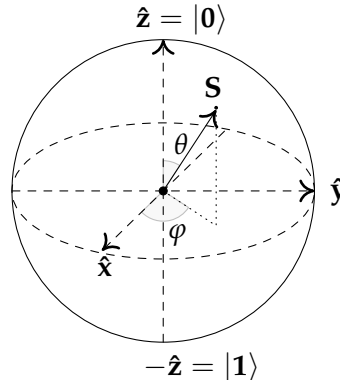


**Figure 4:** The Bloch sphere with a state $|\psi\rangle$ as a vector of a linear combination of $(\hat{x}, \hat{y}, \hat{z})$, with $\hat{z}$ being pure eigenstates and $\hat{x}, \hat{y}$ being complex super positions

tool to visualize two-level systems is the nature of unitary operations. It corresponds to a rotation of the subspace of the Hilbert space that contains the state about one, two or three axis, depending on the euler angles employed for the rotation.

## 8.D The Stoke phase

This thesis will not go to much into the description of the Stoke phase; it is the result of a much more general phenonema. The Stoke phase or Stoke's phenomenon is a result of the asymptotic behaviour of the dispersion relations [26, 32, Sec. Introduction].

**The differential equation:** Let's take a look at the second order differential derived in Eq. 2.6

$$\partial_t^2 A_+(t) = -\partial_t\left[\langle\psi_+|\partial_t\psi_-\rangle\right]A_-(t)e^{2i\int^t dt' E_+(t')} + \langle\psi_+|\partial_t\psi_-\rangle\langle\psi_-|\partial_t\psi_+\rangle A_+(t) + 2iE_+(t)A_+(t) \tag{8.D.1}$$

---

[2]Hyperspheres are also a thing but then the intuition goes out the window. For our system we only need the understanding of $S^2$

Now we realize that we can substitute the $A_-$ coefficient, due to the facts that:

$$\langle\psi_+|\partial_t\psi_-\rangle = \begin{cases} \partial_t\theta_S = -\dfrac{Fk_{0,\Gamma}^2}{F^2t^2 + k_{0,\Gamma}^4} & \text{move } k_z, \text{ displace } k_y/k_x \\[2ex] \partial_t\theta_S = \dfrac{2F^2k_{0,z}t}{k_{0,z}^2 + F^4t^4} & \text{move } k_x, \text{ displace } k_z \\[2ex] \partial_t\phi_S = -\dfrac{2Fk_{0,y}}{k_{0,y}^2 + F^2t^2} & \text{move } k_x, \text{ displace } k_y \end{cases} \tag{8.D.2}$$

$$\partial_t\left[\langle\psi_+|\partial_t\psi_-\rangle\right] = \begin{cases} -\dfrac{2F^2t}{F^2t^2 + k_{0,\Gamma}^4}\partial_t\theta_S & \text{move } k_z, \text{ displace } k_y/k_x \\[2ex] \dfrac{k_{0,z}^2 - 3F^4t^4}{t(k_{0,z}^2 + F^4t^4)}\partial_t\theta_S & \text{move } k_x, \text{ displace } k_z \\[2ex] -\dfrac{2F^2t}{k_{0,y}^2 + F^2t^2}\partial_t\phi_S & \text{move } k_x, \text{ displace } k_y \end{cases} \tag{8.D.3}$$

Due to the fact that we acquire the same expression with a prefactor, we can exchange the first term on the RHS of Eq. 8.D.1 with $\partial_t A_+$,

$$\partial_t^2 A_+(t) = C(t)\partial_t A_+(t) + \langle\psi_+|\partial_t\psi_-\rangle\langle\psi_-|\partial_t\psi_+\rangle A_+(t) + 2iE_+(t)A_+(t), \tag{8.D.4}$$

where $C(t)$ is the prefactor derived in Eq. 8.D.3. What we obtain is a secondary partial differential equation:

$$\partial_t^2 A_+(t) - C(t)\partial_t A_+(t) - D(t)A_+(t) = 0, \tag{8.D.5}$$

where $D(t) = \langle\psi_+|\partial_t\psi_-\rangle\langle\psi_-|\partial_t\psi_+\rangle + 2iE_+(t)$. Remember that,

$$\langle\psi_+|\partial_t\psi_-\rangle = \begin{cases} -\langle\psi_-|\partial_t\psi_+\rangle & \text{move } k_z(k_x), \text{ displace } k_y/k_x(k_z) \\ +\langle\psi_-|\partial_t\psi_+\rangle & \text{move } k_x, \text{ displace } k_y \end{cases}. \tag{8.D.6}$$

In the standard LZ calculations, the second order differential is solved with an expansion in parabolic cylinder functions. The differential equation's exact solutions are matched with that of the asymptotic case far from the crossing (adiabatic). The adiabatic wavefunction solution, $|\psi_{ad}(t)\rangle$ at adiabatic times, $-t_a$ and $t_a$ cf. before and after the crossing then evolves, past the node at time $t = 0$ with a non-adiabatic transition,

$$|\psi_{ad}(t_a)\rangle = U(t_a; 0^+)NU(0^-; -t_a)|\psi_{ad}(-t_a)\rangle, \tag{8.D.7}$$

where $N = M_{LZ}$ is the non-adiabatic transition matrix and $U(t_1; t_2)$ involves the adiabatic dynamics of the wavefunction moving from and to the Weyl node. A Stoke phase appears from this[26].

The solution to this general case, of the differential Eq. 8.D.5 is left to further research. The first order differential persists due to the non-linearity of the coupling of the adiabatic eigenstates. The problem is further complicated by the singular nature of $C(t)$ and $D(t)$. The solution of this is left for further research. If the coefficients have regular singular poles, then the differential equation is Fuchsian, and could likely be solved with the Frobenius method by appying Fuch's theorem, which is closely linked to the Laurent series of the function.

**Timeordered integral and unitary transformations:** Without solving Eq. 8.D.5, we are able to see the relation between the matrices. We set $\alpha = \beta$ in the Hamiltonian for each of the nodes in Eq. 3.1. We write the positive topological charge as,

$$H^+(t) = H^+(k_x(t), k_y) = \Lambda_x(\mathbf{k}(t))\sigma_x + \Lambda_y(\mathbf{k}(t))\sigma_y, \tag{8.D.8}$$

with $\Lambda_x = (k_x(t)^2 - k_y^2)$ and $\Lambda_y = -2k_x(t)k_y$. We then consider the unitary matrix that evolves the state past the node to the times, $t_1$ and $t_2$, which are far from the node,

$$U^+(t_2; t_1) = \mathcal{T}e^{-i\int_{t_1}^{t_2} dt H^+(t)}, \tag{8.D.9}$$

with the ordered exponential integral $\mathcal{T}$. The Hamiltonian for the other node can be written

$$H^-(t) = H^-(k_x(t), k_y) = \Lambda_x(\mathbf{k}(t))\sigma_x - \Lambda_y(\mathbf{k}(t))\sigma_y. \tag{8.D.10}$$

The idea is to realize that $H^+(t) = (H^-(t))^*$, which ultimately leads to the unitary matrix for evolution past the node with a negative charge:

$$U^-(t_2; t_1) = \mathcal{T}e^{-i\int_{t_1}^{t_2} dt H^-(t)} = \mathcal{T}e^{-i\int_{t_1}^{t_2} dt(H^+(t))^*} \tag{8.D.11}$$

Then we can realize that the complex conjugation corresponds to the unitary transformation of the Hamiltonian by the $\sigma_y$-matrix

$$(H^+(\mathbf{k}(t)))^* = -\sigma_y H^+(\mathbf{k}(t))\sigma_y = -\sigma_y \Lambda_x(\mathbf{k}(t))\sigma_x\sigma_y - \sigma_y\Lambda_y(\mathbf{k}(t))\sigma_y\sigma_y = \Lambda_x(\mathbf{k}(t))\sigma_x - \Lambda_y(\mathbf{k}(t))\sigma_y \tag{8.D.12}$$

Equipped with the equality, $H^-(\mathbf{k}(t)) = -\sigma_y H^+(\mathbf{k}(t))\sigma_y$ we rewrite the untary matrix:

$$U^-(t_2; t_1) = \mathcal{T}e^{-i\int_{t_1}^{t_2} dt H^-(t)} = \mathcal{T}e^{i\int_{t_1}^{t_2} dt\sigma_y H^+(t)\sigma_y} \tag{8.D.13}$$

Using again the fact that $\sigma_y\sigma_y = \mathcal{I}_{2\times 2}$

$$\mathcal{T}e^{i\int_{t_1}^{t_2} dt\sigma_y H^+(t)\sigma_y} = \sigma_y \mathcal{T}e^{i\int_{t_1}^{t_2} dt H^+(t)}\sigma_y = \sigma_y(U^+)^{-1}\sigma_y = \sigma_y(U^+)^\dagger\sigma_y \tag{8.D.14}$$

The last equality is due to unitarity. The last step is to realize that $U^\pm = M_{LZ}^\pm$

$$M_{LZ}^- = \begin{pmatrix} \sqrt{P_{LZ}^- - 1}e^{-i(\phi_{St}^- - \pi/2)} & -\sqrt{P_{LZ}^-} \\ \sqrt{P_{LZ}^-} & \sqrt{P_{LZ}^- - 1}e^{i(\phi_{St}^- - \pi/2)} \end{pmatrix} = \sigma_y \begin{pmatrix} \sqrt{P_{LZ}^+ - 1}e^{-i(\phi_{St}^+ - \pi/2)} & -\sqrt{P_{LZ}^+} \\ \sqrt{P_{LZ}^+} & \sqrt{P_{LZ}^+ - 1}e^{i(\phi_{St}^+ - \pi/2)} \end{pmatrix}^\dagger \sigma_y$$

$$= \sigma_y \begin{pmatrix} \sqrt{P_{LZ}^+ - 1}e^{-i(\phi_{St}^+ - \pi/2)} & \sqrt{P_{LZ}^+} \\ -\sqrt{P_{LZ}^+} & \sqrt{P_{LZ}^+ - 1}e^{i(\phi_{St}^+ - \pi/2)} \end{pmatrix} \sigma_y = \sigma_y \begin{pmatrix} i\sqrt{P_{LZ}^+} & -i\sqrt{P_{LZ}^+ - 1}e^{-i(\phi_{St}^+ - \pi/2)} \\ i\sqrt{P_{LZ}^+ - 1}e^{i(\phi_{St}^+ - \pi/2)} & i\sqrt{P_{LZ}^+} \end{pmatrix}$$

$$= \begin{pmatrix} \sqrt{P_{LZ}^+ - 1}e^{i(\phi_{St}^+ - \pi/2)} & -\sqrt{P_{LZ}^+} \\ \sqrt{P_{LZ}^+} & \sqrt{P_{LZ}^+ - 1}e^{-i(\phi_{St}^+ - \pi/2)} \end{pmatrix} \tag{8.D.15}$$

The conclusion is that the Stoke phase of the two are the same exact except for a phase of $\pi$

## 8.E Expanding an elliptic integral, moving in $k_x$ displaced in $k_z$

The integration of the squareroot of a quartic polynomial is an incomplete elliptical integral of the first kind,

$$I_{3\pi/4} = \int_0^{t_0} dt \sqrt{k_{0,z}^2 + F^4 t^4} = \frac{2k_{0,z}\sqrt{ik_{0,z}}}{3F} F\left(i\sinh^{-1}(1)\Big| -1\right), \tag{8.E.1}$$

with $t_0 = e^{3i\pi/4}\frac{\sqrt{k_{0,z}}}{F}$ and,

$$F(\phi|m) = \int_0^\phi d\theta \frac{1}{\sqrt{1 - m\sin^2(\theta)}} \tag{8.E.2}$$

While for $t_0 = e^{i\pi/4} \dfrac{\sqrt{k_{0,z}}}{F}$

$$I_{\pi/4} = \int_0^{t_0} dt \sqrt{k_{0,z}^2 + F^4 t^4} = \frac{(-1)^{1/4} \sqrt{\pi} (|k_{0,z}|)^{3/2}}{8F} \frac{\Gamma(1/4)}{\Gamma(7/4)}. \tag{8.E.3}$$

We will express the elliptical integral in terms of Legendre polynomials, $P_n[x]$ [33, $1^{st}$ Section]. To do this the integral is written a bit differently,

$$F(\phi|m) = 2 \int_0^{\tilde{v}} \frac{dv}{\sqrt{1 + 2\lambda v^2 + v^4}}, \tag{8.E.4}$$

with $v = \tan \dfrac{\theta}{2}$, $\tilde{v} = \tan \dfrac{\phi}{2}$, $\lambda = m' - m$, and $m' = 1 - m$ then,

$$F(\phi|m) = 2 \int_0^{\tilde{v}} dv \sum_{n=0}^{\infty} P_n(-\lambda) v^{2n} \tag{8.E.5}$$

$$= 2 \sum_{n=0}^{\infty} P_n(-\lambda) \frac{(i \tanh[\sinh^{-1}(1)/2])^{2n+1}}{2n+1}. \tag{8.E.6}$$

Now we calculate $\lambda$

$$m = -1 \Rightarrow m' = 2 \Rightarrow \lambda = 1 \tag{8.E.7}$$

$$F(\phi|m) = 2 \sum_{n=0}^{\infty} P_n(-1) \frac{(i \tanh[\sinh^{-1}(1)/2])^{2n+1}}{2n+1} \tag{8.E.8}$$

Numerically it can be checked that,

$$\Re\left[ \frac{4\sqrt{i}}{3} \cdot \sum_{n=0}^{\infty} P_n(-1) \frac{(i \tanh[\sinh^{-1}(1)/2])^{2n+1}}{2n+1} \right] = -\Re\left[ \frac{(-1)^{1/4} \sqrt{\pi}}{8} \frac{\Gamma(1/4)}{\Gamma(7/4)} \right], \tag{8.E.9}$$

$$\Im\left[ \frac{4\sqrt{i}}{3} \cdot \sum_{n=0}^{\infty} P_n(-1) \frac{(i \tanh[\sinh^{-1}(1)/2])^{2n+1}}{2n+1} \right] = \Im\left[ \frac{(-1)^{1/4} \sqrt{\pi}}{8} \frac{\Gamma(1/4)}{\Gamma(7/4)} \right], \tag{8.E.10}$$

or

$$\frac{4\sqrt{i}}{3} \cdot \sum_{n=0}^{\infty} (-1)^n P_n(1) \frac{\left( i \tanh \left[ \frac{\sinh^{-1} 1}{2} \right] \right)^{2n+1}}{2n+1} = -\left[ \frac{(-1)^{1/4} \sqrt{\pi}}{8} \frac{\Gamma(1/4)}{\Gamma(7/4)} \right]^*. \tag{8.E.11}$$

## 8.F   Non-zero temperatures

Until now we have only been concerned with what corresponds to a single particle traveling through the bandstructure. This case is analagous to a Bose-Einstein condensate (BEC) at zero temperature. Instead, to better illustrate the transfer of particles as a function of displacement $k_{0,i}$, we introduce a non-zero temperature, and observe how a Fermi-Dirac (F-D) and Bose-Einstein (B-E) distribution evolve after an evolution through the entirety of the first BZ. Note that this description is for non-interacting particles. The two distributions a given by the eqautions,

$$n_{F-D} = \frac{1}{e^{(E-\mu)/(k_B T)} + 1}, \qquad\qquad n_{B-E} = \frac{1}{e^{(E-\mu)/(k_B T)} - 1} \tag{8.F.1}$$

To demonstrate the displacement dependecy we have plotted the distribution and the tranfered fraction in Fig. 5
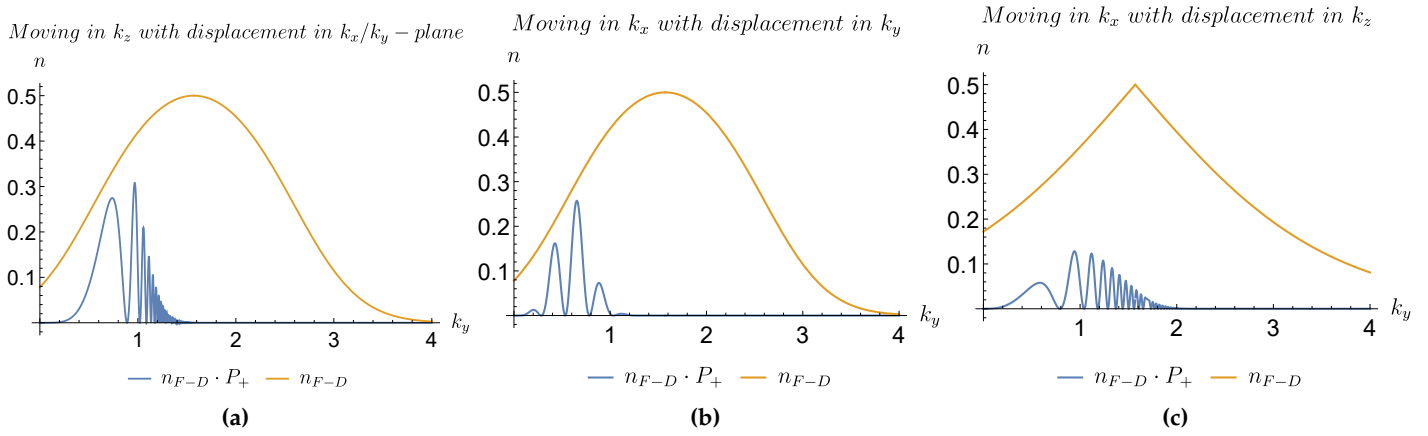
**Figure 5:** The Fermi-Dirac distribution and the amount that is transfered in the three cases for F=1.

## 8.G  Higher order correction plots

In this section we will plot the integrals as a function of $\omega_i$. To obtain a numerically graphable function from Mathematica it is advisable to write the exponential as the followin instead,

$$\int_0^\infty dt e^{\pm(t^3 \pm (\omega_j - \omega_{j-1}))} = \int_0^\infty dt \cos(t^3 \pm (\omega_j - \omega_{j-1})) \pm i \sin(t^3 \pm (\omega_j - \omega_{j-1})). \tag{8.G.1}$$

The two solutions are,

$$\frac{\pi}{\sqrt[3]{3}} \text{Ai}\left[\pm \frac{\omega}{\sqrt[3]{3}}\right] \pm \frac{i}{360}\left[40 \cdot \sqrt[3]{3}^2 \text{Bi}\left[\pm \frac{\omega}{\sqrt[3]{3}}\right] - 60\omega^2 {}_1F_4\left[1; \frac{2}{3}, \frac{5}{6}, \frac{7}{6}, \frac{4}{3}; \frac{\omega^6}{108^2}\right] \mp \omega^5 {}_1F_4\left[1; \frac{7}{6}, \frac{4}{3}, \frac{5}{3}, \frac{11}{6}; \frac{\omega^6}{108^2}\right]\right]. \tag{8.G.2}$$



(a)



(b)





28
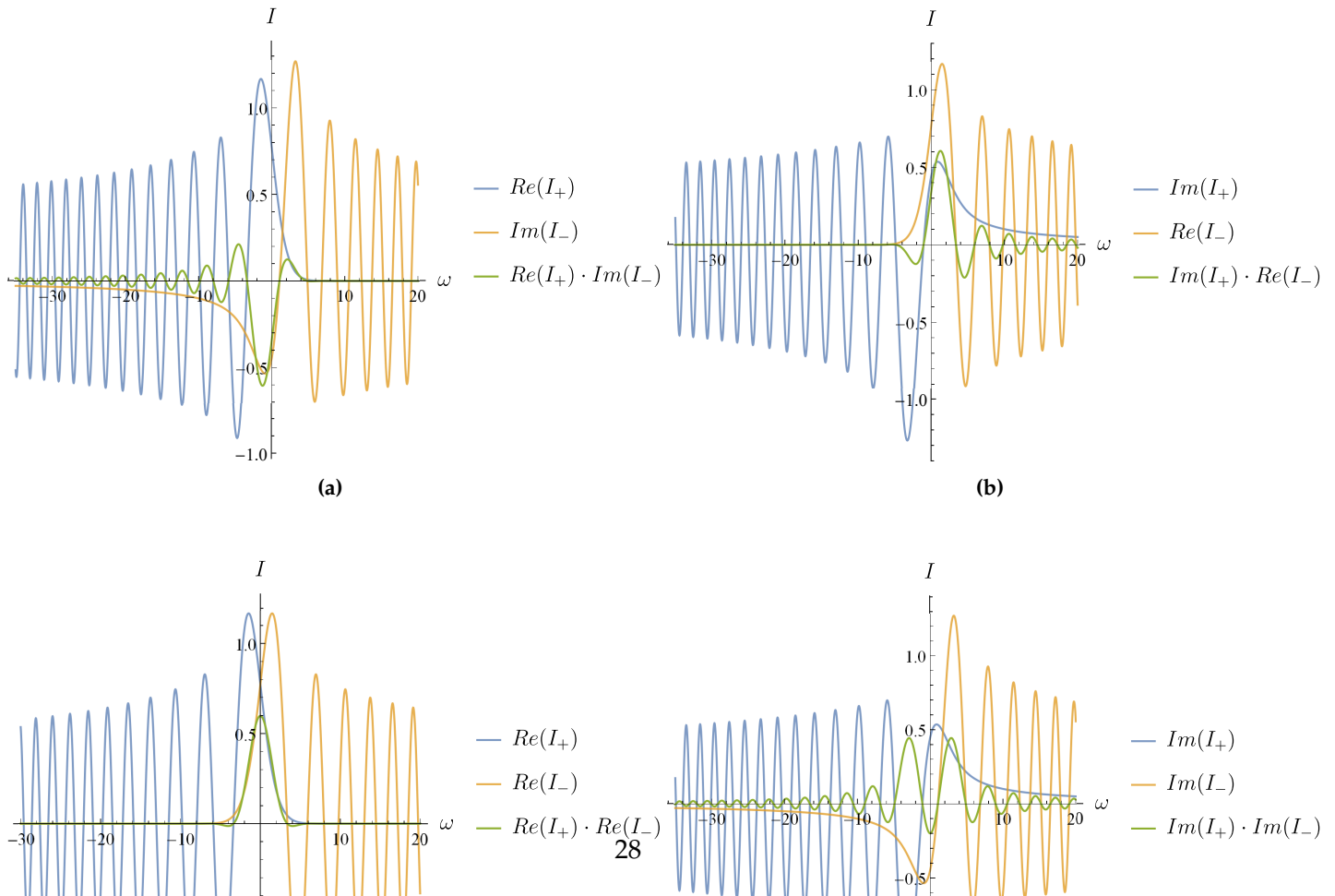
## 8.H  The Berry curvature and flux calculations

The Berry flux, also called the Chern number or chirality, is found by integrating a sphere, $d\mathbf{S}$, enclosing the node in momentum space over the Berry curvature,

$$C = \frac{1}{2\pi} \int_S \mathbf{\Omega} \cdot d\mathbf{S_k}. \tag{8.H.1}$$

The normal of a sphere is naturally the radial unit vector and the infitisimal area is given as $dA = k^2 \sin(\theta) d\phi d\theta$,

$$C = \int_0^\pi \int_0^{2\pi} \frac{1}{k^2 \sin(\theta_k)} \partial_{\theta_k}(\cos\theta_S) k^2 \sin(\theta_k) d\phi d\theta = 2\pi \int_0^\pi \partial_{\theta_k} \cos(\theta_S) d\theta_k = 2\pi \left( \frac{k\cos(\theta_k)}{k\sqrt{\cos^2(\theta_k) + k^2 \sin^4(\theta_k)}} \right) \Bigg|_0^\pi$$

$$= -4\pi. \tag{8.H.2}$$

This is a double-Weyl point sink, with a topological charge of $-2$. The same flux can be found for the Berry curvature in Cartesian coordinates. Instead of a sphere, infinitely large planes seperated from the monopole by some constant number has to be integrated.

$$C = \iint_{-\infty}^\infty dk_i dk_j \Omega_k(K_k^+, k_i, k_j) - \iint_{-\infty}^\infty dk_i dk_j \Omega_k(K_k^-, k_i, k_j) \tag{8.H.3}$$

This is the same as integrating a box in Cartesian coordinate space with sidelengths, $L = k_{x/y/z}^+ - k_{x/y/z}^-$. No matter the axis that these planes are perpendicular to, the flux through is of the size $4\pi$.

$$\int_{-\infty}^\infty dk_z \Omega_x(K_x^+, k_y, k_z) = \frac{k_x - k_y \frac{S_y}{S_x}}{S_x\left(\frac{S_y^2}{S_x^2} + 1\right)} \left[\frac{k_z}{E_+}\right]_{-\infty}^\infty ; \quad \int_{-\infty}^\infty dk_z \Omega_y(K_y^+, k_x, k_z) = -\frac{k_y - k_x \frac{S_y}{S_x}}{S_x\left(\frac{S_y^2}{S_x^2} + 1\right)} \left[\frac{k_z}{E_+}\right]_{-\infty}^\infty \tag{8.H.4}$$

Evaluation of the integral yields,

$$\lim_{k_z \to \pm\infty} \left[\frac{k_z}{E_+}\right] = \lim_{\theta_S \to 0 \vee \pi} \left[\cos(\theta_S)\right] = \pm 1. \tag{8.H.5}$$

Before integrating the $k_y, k_x$ dependent terms, note that,

$$\frac{k_x - k_y \frac{S_y}{S_x}}{S_x\left(\frac{S_y^2}{S_x^2} + 1\right)} = -\frac{1}{2}\left(\frac{dS_x}{dk_y}\frac{d\phi_S}{dS_x} + \frac{dS_y}{dk_y}\frac{d\phi_S}{dS_y}\right), \qquad -\frac{k_y - k_x \frac{S_y}{S_x}}{S_x\left(\frac{S_y^2}{S_x^2} + 1\right)} = -\frac{1}{2}\left(\frac{dS_x}{dk_x}\frac{d\phi_S}{dS_x} + \frac{dS_y}{dk_x}\frac{d\phi_S}{dS_y}\right). \tag{8.H.6}$$

This yields,

$$\iint_{-\infty}^\infty dk_y dk_z \Omega_x(K_x^\pm, k_y, k_z) = \int_{-\infty}^\infty dk_y \frac{1}{2}\frac{d\phi_S}{dk_y}\left[\frac{k_z}{E_+}\right]_{-\infty}^\infty = 2K_x^+ \int_{-\infty}^\infty dk_y \frac{1}{k_x^2 + k_y^2} = \pm 2\pi.$$

The same method yields the same result for $\iint_{-\infty}^\infty dk_x dk_z \Omega_y(K_y^\pm, k_x, k_z)$. For $\Omega_z$-component,

$$\iint_{-\infty}^\infty dk_x dk_y \Omega_z(K_z^+, k_y, k_x) = \int_{-\infty}^\infty dk_y [A_y(\mathbf{k})]_{-\infty}^\infty - \int_{-\infty}^\infty dk_x [A_x(\mathbf{k})]_{-\infty}^\infty \tag{8.H.7}$$

Note that this is equal to zero. In the integration we need to account for poles,

$$\iint_{-\infty}^\infty dk_x dk_y \left[\partial_{k_x} A_y - \partial_{k_y} A_x\right]. \tag{8.H.8}$$

The result is a Chern number of $-4\pi$. In Fig. 7 we have plotted the stream lines of the Berry curvature of Eq. 4.9. From this we can see that in the vicinity of $\mathbf{k} = (0,0,0)$ the node changes the direction of the stream line going in the $k_z$ direction. This is the reason that the integration of the infinite plane perpendicular to the $k_z$-axis yields a pole .

**Figure 7:** The Berry curvature field lines. c) shows the lines seen from $k_z = 0$. Altering $k_z$ does not change the field lines only the strenght of them. The 4 grid lines show where the slices a,b,d,e) are from. a,b,d,e) shows the deoendency of the orientation by the position $k_x, k_y$. The field lines point either up or down in $k_z$